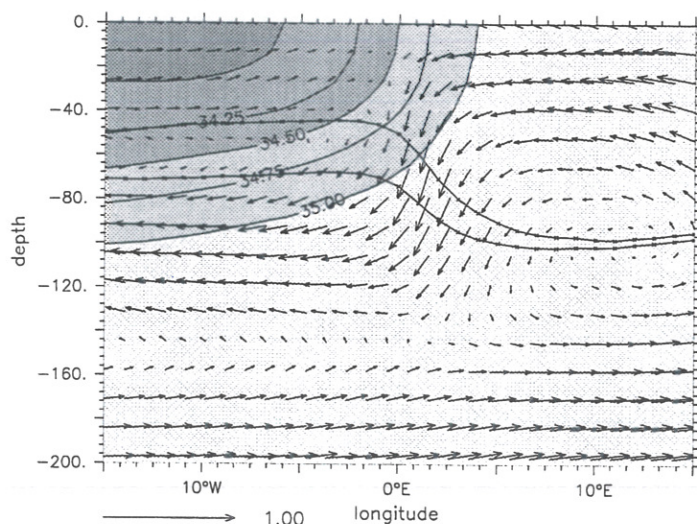# Institut Pierre Simon Laplace
des Sciences de l'Environnement Global

Notes du Pôle de Modélisation

An OGCM Study for the TOGA Decade.
Part I: Role of Salinity in the Physics of the Western Pacific Fresh Pool,
Part II: Barrier layer formation and variability

Jérôme Vialard et Pascale Delecluse

Laboratoire d'Océanologie DYnamique et de Climatologie

Mars 1998   **Note n° 4**

An OGCM Study for the TOGA Decade.
Part I: Role of Salinity in the Physics of the Western Pacific Fresh Pool,
Part II: Barrier layer formation and variability
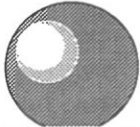
Jérôme Vialard et Pascale Delecluse

Laboratoire d'Océanologie DYnamique et de Climatologie

Ce travail vise à évaluer l'importance de la structure haline très spécifique du Pacifique Ouest dans l'équilibre thermique et dynamique de celui ci, en s'appuyant sur des expériences numériques avec un modèle de circulation générale océanique. La barrière de sel est une couche d'eau chaude et stratifiée en sel, située entre les eaux de surface du Pacifique Ouest et celles plus froides de la thermocline. Une étude en mode forcé permet d'étudier les mécanismes de formation de cette structure. La pénétration du flux solaire contribue à la maintenir, mais c'est la dynamique tridimensionnelle qui fournit l'apport d'eau chaude et salée en subsurface nécessaire à sa formation. Dans la bande équatoriale, ce processus de subduction est lié au front de salinité, conséquence de la convergence zonale des eaux salées du Pacifique central et des eaux douces du Pacifique Ouest. La structure haline contribue activement à ce mécanisme, en piégeant la quantité de mouvement des vents d'Ouest dans la couche de surface du Pacifique Ouest, accentuant ainsi la convergence zonale des courants. Le downwelling associé à cette convergence alimente la subsurface du Pacifique Ouest en eau chaude et salée. Au sud de l'équateur, le mécanisme de subduction mis en évidence s'apparente à celui proposé par Shinoda et Lukas (1995). ../..

Mars 1998
Note n° 4

L'impact de la barrière de sel sur le bilan thermique est double. D'une part, son effet isolant diminue le refroidissement par entraînement des eaux de surface. D'autre part, la stratification haline limite la profondeur de la couche de mélange, et donc la quantité de flux solaire pénétrant intercepté par celle ci. La manière dont ces deux effets se compensent est toutefois sensible aux forçages utilisés, et difficile a evaluer. La barrière de sel pourrait en revanche jouer un rôle dans la variabilité interannuelle du système couplé : les coups de vent d'Ouest aboutissent à la formation de barrière de sel épaisse dans le Pacifique Central. L'évaluation de la réponse locale et grande échelle du système océan atmosphère à cette formation de barrière de sel ne peut toutefois être réellement évaluée que dans le cadre d'expériences couplées.

An OGCM Study for the TOGA Decade.
Part I: Role of Salinity in the Physics
of the Western Pacific Fresh Pool

Jérôme Vialard and Pascale Delecluse
Laboratoire d'Océanographie DYnamique et de Climatologie (LODYC)
Case 100, Université Pierre et Marie Curie
4, Place Jussieu - 75252 Paris Cedex 05 - France

Revised version

Abstract

A set of numerical simulations of the tropical Pacific Ocean during the 1985 - 1994 decade is used to investigate the effects of haline stratification on the low frequency equilibrium of the COARE region. The simulated SSS structure is found to be quite sensitive to the freshwater forcing, and to the other fluxes. Despite this sensitivity, several robust features are found in the model. Sensitivity experiments illustrate the important role of the haline stratification in the western Pacific. This stratification is the result of a balance between precipitations and entrainment of subsurface saltier water. It inhibits the downward penetration of turbulent kinetic energy. This results notably in a trapping of the westerly wind bursts momentum in the surface layer, giving rise to strong fresh equatorial jets.

The model is able to produce barrier layer between 5°N and 10°S in the western Pacific and under the inter tropical convergence zone, like in Ando and McPhaden (1997) composites, but also around 120°W, 10°S, where there is no data to validate its presence. The barrier layer thickness in these regions is found to be sensitive to local water forcing, and its spatial structure is governed by the large scale circulation. The heat budget of the upper ocean mixed layer is analyzed in these barrier layer regions. Lukas and Lindstrom (1991) hypothesis that the surface heat flux should be near zero in these regions in order to maintain the weak temperature gradient between the mixed layer and the barrier layer does not seems necessary. A significant part of the solar heat flux is lost beneath the thin mixed layer, attenuating the heating of the surface layer and allowing barrier layer upholding in presence of a positive net heat flux. Conversely, the development of the barrier layer is associated with a dramatic decrease of the entrainment cooling, or even entrainment heating, especially near the equator. On the whole, the barrier layer seems to insulate the SST from the effects of atmospheric forcing.

Influence de la salinité sur les interactions océan - atmosphère dans le Pacifique tropical.

A.1. Introduction

Recent advances in the understanding of the El Niño / Southern oscillation (ENSO) phenomenon suggest that air sea interactions in the western Pacific (hereafter referred as "WP") are important in the onset of such an event (Lukas, 1988). The atmospheric circulation is indeed very sensitive to the sea surface temperature in this region. The mechanisms driving the variability of temperature are thus essential in the understanding of the coupled ocean - atmosphere system response. At first glance, salinity plays very little role in these coupled interactions. However, it has been suggested that the amount of oceanic heat directly available for the atmosphere in the upper layer of the warm pool can be dependent on the haline stratification. This is due to the so - called phenomenon of "barrier layer" (hereafter referenced as "BL", "BLT" standing for "Barrier layer thickness") (Lukas and Lindstrom, 1991). A BL is present when the isohaline layer is shallower than the isothermal layer (see figure 1). In such a case, the mixed layer depth is controlled by the salinity stratification. The underlying water has a potential temperature close to the SST. A deepening of the mixed layer (under the effect of a wind burst, for example) will not affect surface temperature via entrainment cooling. That is why the water column between the bottom of the mixed layer and the top of the thermocline has been named "barrier layer". Using data from Levitus (1982), the presence of the BL in the three tropical oceans has been recognized to be not just a sporadic event but a climatological feature (Sprintall and Tomczack, 1992). Moreover, a strong time variability of the BL has been observed and linked to interannual variability (Delcroix *et al.*, 1992; Sprintall and McPhaden, 1994).

Several questions arise from the existence of such a structure. First, is it significant enough on the surface layer heat budget to allow the formation of large scale SST warm anomalies? Then, what allows such a structure to appear and to persist on seasonal timescale? In order to maintain a BL, the water of the mixed layer has indeed to stay at the same temperature than the underlying BL. Does the net surface heat flux need to be close to zero in the WP in order to maintain the weak vertical temperature gradient between the surface layer and the BL as suggested by Lukas and Lindstrom (1991)? This study tries to address these questions using OGCM simulations. This paper (part I)

investigates the role of salinity in the physics of the WP warm and fresh pool. The modeling framework and the surface forcings are presented. Of course the large scale modeling technique has its limits and some of them might be reached in this study of the fine mixed layer processes of the WP where high frequency and small scale processes might be important (e.g. Tomczack, 1995; Chen and Rohstein, 1991). Much care will thus be taken in this paper to test the sensitivity of the simulated processes to the forcing and the resolution. Robust results of this study include the trapping of atmospheric fluxes in the surface layer of the warm pool by haline stratification, the role of the penetrative solar heat flux in the heat budget of the upper layers of the WP, and the impact of the BL on entrainment fluxes, especially near the equator. An associated paper (part II) goes more deeply into the details of the large scale BL formation processes and interannual variability.

This paper is organized as follows. Section 2 describes the modeling approach. The simulated circulation and its sensitivity to the forcing and to some model parameters are described in section 3. The sensitivity of the vertical mixing to the haline stratification gives some insights on the role of the salinity in the physics of the warm pool. In section 4, the upper layer structure of the warm pool is examined. A BL structure is found in the model results and its impact on the upper layer heat budget is analyzed. Section 5 summarizes the more important results of this study. The uncertainties and shadow areas that remain are then discussed.

A.2. The modeling approach

A.2.1. The model

The model used for this study is the OPA primitive equation OGCM. It has been developed at LODYC (*Laboratoire d'Océanographie Dynamique et de Climatologie*) by Delecluse's team. The basic assumptions and the set of discretized equations using tensorial formalism are described in Delecluse *et al.* (1993). The main assumptions and parameterizations are summarized here:
- Primitive equations, including potential temperature and salinity.
- Rigid lid approximation on the top.
- Turbulent closure hypothesis: it is assumed that small scale horizontal and vertical transports can be evaluated in terms of diffusion coefficients and derivatives of the large scale flow.

The equation of state is computed from Unesco formulation (Millero and Poisson, 1981). The equations are discretized with a second order finite difference scheme on an Arakawa (1972) C grid. The temporal scheme is a leapfrog scheme with Asselin (1972) filter, except for vertical diffusion which uses an implicit scheme, and the horizontal diffusion which uses a forward scheme.

A.2.2. Adaptation for a tropical Pacific experiment

a) Physics of the model

The LODYC model has been adapted for a medium - resolution simulation of the tropical Pacific ocean circulation by Maes *et al.* (1997), to study the effects of the horizontal diffusion on the large scale patterns of the equatorial dynamics. The domain covers the tropical Pacific between 130 °E and 75°W, and between 30°N and 30°S. It has a 1° zonal resolution and a meridional resolution varying from 0.5° at the equator to 2° at the northern and southern boundaries. The vertical resolution varies from 10 meters in the 120 first meters up to 1 kilometer at depth (20 levels). A time step of 5400 seconds (1.5 hour) is used.

No-slip boundary conditions and no flux conditions for heat and salt are applied at the bottom and along the coastlines and boundaries. A damping towards Levitus (1982) monthly temperature and annual salinity is used near the southern and northern boundaries, in order to take care of fluxes into and out of the domain. In the 20°N - 20°S band, the ocean is left free.

We use in this study a Laplacian horizontal diffusion with a constant coefficient of 10^3 m^{2}s^{-1} (see Maes *et al.* (1997) for a detailed discussion of the sensitivity of the model results to the choice of this coefficient). The vertical eddy coefficients are computed from a 1.5 turbulent closure model in which the evolution of the turbulent kinetic energy is given by a prognostic equation (Blanke and Delecluse, 1993).

We want to study fine scale mixed layer processes in the WP. Resolution is of primary importance for these processes. Vertical resolution is important to capture the vertical stratified (e.g., Tomczack, 1996) and sheared (McPhaden *et al.*, 1992) structure of the warm pool. Horizontal resolution should also try to capture at best the fine scale horizontal structures that can appear in the warm pool. We have thus tested the sensitivity of our model results to the use of higher resolutions (see table

1 for a summary of the sensitivity experiments used in this study). The model was run with a 5 meter vertical resolution from the surface to 120 meter depth (table 1, experiment A7). After three years of spin up, the results of the A7 and C experiments were compared for the year 1985. Differences are weak (figure not shown). Furthermore, they appear mostly in the central Pacific where A7 displays a 10 meters shallower mixing layer depth than C (control experiment) in the vicinity of the equator. This is presumably due to a different representation of the shear in the transition zone between the South Equatorial Current (SEC) and the Equatorial UnderCurrent (EUC). The OPA model has also been adapted by Maes (1996) for a high resolution study of the three tropical oceans (with a 0.33° meridional resolution at the equator, a zonal resolution between 0.33° and 0.75° and 30 levels). Experiment H1 of his model is similar to our control experiment in every respect except resolution. Experiments C and H1 display very similar results. The choice of the horizontal and vertical resolution is thus a good compromise between model performance and computational cost.

b) The forcing

We used daily forcing issued from the Arpege Atmospheric General Circulation Model (AGCM) AMIP T42L30 experiment (Déqué *et al.*, 1994; Déqué, 1995). Surface fluxes of momentum, heat and salinity are prescribed through the use of wind stress, fresh water budget and net heat flux at the sea surface:

$$\left(K_m \partial_z \vec{U}_h\right)_{z=0} = \vec{\tau} / \rho_0$$

$$\left(K_\rho \partial_z S\right)_{z=0} = (e - p)S$$

$$\left(K_\rho \partial_z T\right)_{z=0} = \left(Q^* + \gamma(T - T^*)\right)/\left(\rho_0 C_p\right)$$

where $\vec{U}_h$ is the horizontal projection of velocity, T the temperature, S the salinity, ρ_0 the reference density, C_p the sea water specific heat, K_m and K_ρ respectively the momentum and tracer vertical mixing coefficients, $\vec{\tau}$ the wind stress, e-p the fresh water budget (no run off) and Q^* the non - penetrative part of the surface heat flux. A penetrative solar radiation corresponding to a Jerlov type I water (Jerlov, 1968) is used.

The strong coupling between surface ocean heat loss and SST is approximated by a local restoring term toward observed sea surface temperature T^* (Reynolds and Smith, 1994). In a

forced framework, such a restoring term is needed in order to avoid unrealistic temperatures induced by heat forcing biases. The restoring coefficient $\gamma = \partial_{SST} Q^*$ is taken equal to -40 W.m^{-2}.K^{-1} everywhere. This constant value is chosen because the study made by Oberhuber (1988) for γ gives only slight variations around -40 W.m^{-2}.K^{-1} in the tropics (see Dandin (1993) for a detailed discussion of this value). There is no restoring toward observed sea surface salinity because salinity does not affect directly the air-sea exchanges.

Starting from rest, with Levitus salinity and temperature, the model is spun up during two years with daily forcing obtained by averaging the 1984 - 1993 Arpege forcing, and one more year with simulated wind stress and fluxes from 1984. We assume that the state obtained after this three year spin-up is representative from the state of the ocean at the end of 1984, and the model is integrated during the 1985-1994 decade. This is the control experiment C.

The use of this AGCM forcing is however the source of several questions. First, how realistic are the forcings issued from this AGCM? Second, is the spatial and temporal sampling of the AGCM outputs fine enough to include all the forcings structures that are important to our study? Let us examine what biases might exhibit the Arpege forcing. The figure 2 displays a comparison between the 1985-1994 Arpege forcings and monthly mean observed wind stresses (Hellerman and Rosenstein, 1983, hereafter HR), fresh water budget (Arkin and Ardanuy, 1989) and net surface heat flux (Oberhuber, 1988). One of the biases of Arpege is the eastward shift of the Walker circulation ascending branch. This results first in weak winds in the equatorial band where Arpege wind stresses are less than 0.05 Pa whereas they exceed 0.07 in HR. This feature is associated with a stronger eastward penetration of the Australian monsoon into the WP. Eastward equatorial wind stresses indeed reach the dateline in Arpege annual cycle, whereas they stay west of 160° East in HR. The eastward shift of the convection zone is also associated to a negative evaporation minus precipitations budget extending more toward the central Pacific than in the dataset (the -1 mm/day isohyet reaches 170° West whereas it is near the dateline in data). Convection is not only shifted east but also weaker than in observations, leading to low precipitations over the warm pool (where net water flux is around -3 mm.day^{-1} compared to the -6 mm.day^{-1} value of data).

This is also true in the eastern Inter Tropical Convergence Zone (ITCZ), where Arpege does not exceed 5 mm.day^{-1}, whereas the MSU precipitation product (Spencer, 1993) suggest 11 mm.day^{-1}. Arpege has also a tendency to form a "mirror ITCZ" south of the equator, which is evidenced by occasional freshwater fluxes into the ocean between 160° West and the American coast around 5° South. As many other atmospheric models, the long term estimate of the net heat flux into the ocean is nearly correct, but with both short wave heat gain and latent heat losses overestimated by 40 W.m^{-2} (Dandin, 1993). Finally, the intraseasonal variability of Arpege surface fluxes (and especially wind stress) is underestimated (Slingo et al., 1996). The Arpege surface flux dataset thus displays some identified biases. It was chosen because it provides an interannual high frequency (daily) coherent forcing dataset over the whole Pacific. Furthermore, forcing the model with Arpege was an introductory experiment for further coupled studies.

One might however wonder whether the daily forcing frequency is enough to deal with the BL processes. The BL is indeed closely linked with fine mixed layer processes. Diurnal cycle was suggested to be important in its formation. Chen et Rohstein (1991), for instance, included diurnal cycle in their one - dimensional BL formation model. An experiment was conducted with an idealized short-wave heat flux diurnal cycle computed from Arpege daily forcing (see table 1, experiment A6). The introduction of this diurnal cycle had no effect at all on the simulated mixing layer and BLT. This result has however to be considered with care, relatively to the coarse resolution of the upper ocean layers (10 meters) with respect to the diurnal cycle vertical scale. Tests conducted with a one dimensional (and 0.5 meters vertical resolution!) mixed layer model suggest an explanation to this lack of sensitivity: except just after a strong rain event, the diurnal cycle concerns mainly a 20 meters thick layer situated above the top of the BL (Josse, 1996). The same study however suggests that the occurrence of rainfall at evening or night might have a stronger effect than in the morning.

A.3. Mean simulated circulation

A.3.1. Large scale structure

The general ability of the model to reproduce the large scale major patterns of the equatorial circulation is presented in Maes et al. (1997).

Identical main features are found when considering the mean state of our experiment (east - west thermocline tilting, deep equatorial counter current, etc...), although we use a high frequency interannual forcing. We will not discuss them in this study. As we are interested in the fine thermohaline structure of the upper WP and its driving mechanisms, we have to examine closely the variables controlling its mean state and variability.

As observed by Sprintall and McPhaden (1994), the intensity and reversals of the SEC are crucial in driving the upper ocean structure of the WP, as well as they are in the subduction mechanism proposed by Lukas and Lindstrom (1991) and Shinoda and Lukas (1995). Figure 2 shows a comparison of mean simulated and measured velocity in the surface layer (Reverdin et al., 1995). We can see a good agreement of the measured and simulated mean surface circulation, though the North Equatorial Counter-Current (NECC) looks slightly too weak in the model (which might be partly explained by the weak wind convergence of Arpege in the ITCZ region). The variance of the surface speed (figure not shown) is also in good agreement with data, with slightly too much variability at the equator around the dateline (due to excessive eastward penetration of Arpege westerlies in this region: see part 2.2.b). We can thus hope that the exchanges between the western and central Pacific will be reasonably reproduced in the surface layer.

SSS is the key parameter for the BL. The general structure of the average annual fresh and salty water distributions are roughly reproduced by the model experiment (see figure 2), with fresh water in the ITCZ and South Pacific Convergence Zone (SPCZ) regions and saltier water in the central equatorial Pacific and the eastern subtropical maximum. However, the simulated salinity structure exhibits important biases. The fresh pool of 33 psu water appearing west of the Costa Rican coast is too salty in the model results. The weak precipitations of Arpege there, and the lack of runoff in our model probably explain this overestimated value. On the opposite, regions under the western and central ITCZ and under the SPCZ have very low SSS (with differences up to 1 psu), compared to the annual mean produced by Delcroix et al. (1996). The salinity in the central Pacific is also slightly too low (with equatorial surface maximum around 35 psu instead of 35.3).

In order to understand what drives the SSS equilibrium, we performed an experiment that allowed us to test the sensitivity of the modeled SSS to the water flux. The model was run with the LMD AGCM (Sadourny and Laval, 1984) AMIP experiment freshwater flux (experiment A4) and then with all the LMD fluxes (experiment A5). The LMD water flux has a structure which is much alike the MSU precipitation data, with very strong evaporation compared to Oberhuber (1988) in the subtropics (4 mm.day^{-1} instead of 1) and a convection zone shifted of 2000 kilometers to the west (figure 4a). The modeled SSS reveals itself very sensitive to the water flux with quite different structures and variability in C and A4 (figure 4b). The simulated surface currents are not much changed: the differences between C and A4 are not caused by circulation changes. Experiment A4 has better SSS values near Costa Rican coast (due to stronger LMD precipitations in this region). On the opposite, SSS is overestimated in the subtropics due to excessive evaporation, with values up to 37.2 psu, which is 1 psu more than the observed average (Delcroix et al., 1996). In the ITCZ and SPCZ regions, the improvement of the water flux forcing does not improve the simulated SSS, suggesting that the biases toward low values has another origin than the water flux.

Advection might also be an important term in driving the SSS structure in these regions as suggested by Levitus (85). Experiments H1, H2 and H3 confirm this idea. They exhibit quite different SSS structures whereas they have been produced using the same water flux. The use of different heat fluxes and wind stresses lead to significantly different circulation patterns. In experiment H3, for instance, a stronger NECC leads to a better representation of the SSS in the WP ITCZ region. The forcing associated to these simulations differ by the location of the convective center of the Walker cell. It is situated far east in experiments A5 and H3, resulting in stronger easterlies all over the equatorial band. Experiment H2 stands for an intermediate situation. The easterlies are weaker and reverse over a large portion of the WP in experiment H1. These differences lead to a variable extension of the SEC in the WP in the four experiments. The monthly surface current product of Reverdin et al. (1995) shows an eastward penetration of the SEC which does not cross the dateline in the equatorial band. This feature depends on the wind stress in our experiments. The eastward penetration of the SEC is too strong in experiments H3 and A5 (with westward velocities all through the equatorial Pacific), leading to a penetration of the central equatorial salty water tongue into the WP "fresh water

pool" (we refer hereafter to the <35 psu equatorial water lying between 10°N and 10°S in the WP as the "fresh pool"). On the opposite, the slightly overestimated reverse of the SEC in the WP of experiment H1 result in an eastward shift of this fresh pool. H2 stands as an intermediate. Wind forcing is also an important factor in driving the haline structure of the WP, through its impact upon the zonal extension of the SEC.

Finally, freshly biased surface salinity in our experiments might also be due to weak entrainment of subsurface saltier water in the WP. This might be due to an underestimation of high frequency wind forcing in the AGCM wind stress dataset and to the weak diapycnal mixing in the model. The weak equatorial upwelling also maybe leads to an underestimated salt flux into the surface layer.

Without a damping toward observed SSS, the modeled salinity structure reveals itself very sensitive to the prescribed water budget. It is also sensitive to the wind forcing via the simulated circulation. Despite this sensitivity, our modeling results were robust to most changes in the surface forcing.

A.3.2. Sensitivity of the circulation to the salinity effects in the vertical mixing

We try in this chapter to investigate the impact of haline stratification on the equilibrium of the warm pool. Via its effect in the equation of state, the salinity indeed contributes to the vertical stratification, and thus to the turbulent kinetic energy dissipation. Miller (1976) used a one-dimensional mixed layer model to show that the inclusion of salinity could modify the surface layer heat balance by inhibiting the vertical mixing. To understand the impact of salinity stratification on the vertical fluxes in the upper layers, an experiment is conducted where the turbulent processes are solved without considering the salinity stratification. This can be done in the model by computing the potential density as a function of temperature only (salinity was fixed to 35.5 psu in the equation of state). The potential density is indeed used to evaluate the turbulent kinetic energy dissipation / production by the stratification (Blanke and Delecluse, 1993). Resolution is otherwise conducted as usual, including the salinity prognostic equation. This simulation is referred as A1.

Experiment A1 reveals several major differences with the control experiment. The figure 5a displays the difference of the modeled

mixing layer depth (defined as the layer with a vertical diffusion coefficient larger than 5.10^{-4} $m^2.s^{-1}$) between experiments C and A1. The figure 5b displays the surface zonal current difference. In these equatorial WP, neglecting salinity effects results in a deeper mixing layer in A1. Salinity increases the vertical stratification, and opposes the penetration of turbulent kinetic energy into the ocean associated to wind stirring or convective events. Both atmospheric water and momentum fluxes are thus distributed over a thicker ocean layer in A1 experiment, which results in a saltier water in the WP. The westerly wind stresses that blow west of the dateline during the Australian monsoon, westerly wind bursts or El Niño events are also distributed over a thicker layer, resulting in weaker surface jets in A1. This ends up in average westward currents all through the equatorial band in A1 experiment, whereas the surface flow is on the average eastwards west of the dateline in the control experiment (see figure 5b). Furthermore, the inclusion of the salinity results in stronger zonal current variability (associated to eastward jets) as can be spotted from the zonal speed variance over the C and A1 experiments (figures not shown). By trapping the westerly wind stresses in the surface layer of the fresh pool, the salinity seems to have an active effect in the zonal advection, which in turn is determinant for the warm and fresh pool displacements (Picaut et al., 1996; Delcroix and Picaut, 1997). The asymmetry in the haline effect on the response of the upper ocean in this region (the trapping of the westerly stresses being more effective than the trapping of easterly stresses) might be explained by nonlinear effects. The meridional convergence indeed traps the zonal momentum near the equator in an eastward jet whereas the momentum diverges away from it in a westward current.

Salinity thus traps the atmospheric fluxes in the surface layer of the warm pool by controlling the mixing layer depth in this weakly thermally stratified region. The salinity stratification might actively contribute to the warm pool equilibrium by helping to set up the zonal convergence which drives its eastern edge position (Picaut et al, 1996). It is however difficult to fully assess the role of the salinity in the warm pool equilibrium in this forced framework, because of the damping toward the observed SST. The modeled warm pool is indeed constrained to stay close of the observed one because of this corrective surface heat flux.

A.4. Upper layer structure in the western Pacific fresh pool

A.4.1. Horizontal distribution of barrier layer

The model results have been used to map a mean BLT in the Pacific ocean, as well as its variance (see Figure 6a and 6b). The criterion we use to compute the BLT is the one used by Sprintall et Tomczack (1992). In their study, the BLT is determined by the difference between the depth of the (SST - 0.5°C) isotherm and the depth of (sea surface density + $\partial\rho/\partial T(SST,SSS)*(-0.5°C)$) isopycn, representative of the salinity stratification accounting for the same density change than a 0.5°C temperature variation. It has been chosen because the vertical resolution of the model (10 meters in the surface layers) does not allow to use the vertical gradient criterion of Lukas and Lindstrom (1991). However, both criteria give similar results with measured profiles (Ando and McPhaden, 1997, hereafter referenced as AM).

The mean simulated BLT over the 85-94 period (Figure 6a) is in good agreement with the composite for normal years of AM (figure 6c). The thickest BLs occur in the equatorial region, in a 10°S - 5°N latitude range and between 140°E - 170°W. Two areas of thick BLT and strong BLT variability can be distinguished in this region: one at the equator and the other in the 3°S - 7°S band (figure 6a and b). The root mean square of the simulated BL in both these regions is of the same order than the mean BL itself, suggesting it can sometimes totally disappear.

We will now explore the differences between our results and AM analysis. A BL also appears in the southeastern part of the basin in our study (around 120°W, 12°S) but is missing from AM composites. This region is however situated in a gap between available data points. It is thus difficult to say whether modeled thick BLs there exist. This BL formation region is not simply the result of Arpege "mirror ITCZ". It is indeed a robust feature of the results when using a different fresh water budget (experiment A4, for instance). The simulated BL field is systematically thinner than the measured one. In the equatorial region west of the dateline, the modeled BL ranges from 10 to 15 meters whereas AM composite ranges from 20 to 30 meters. Additionally, a 10 meter thick BL extends eastward to 120°W under the ITCZ,

whereas our control experiment does not display such a thick BL in this region.

Several experiments allow us to test the sensitivity of the BL to the wind and heat forcing. A recent work by Maes (1996) suggests that the high frequency variations (2-60 days) of the wind stress are important to remove heat out of the warm pool. The H1 and H2 experiments use the same water flux (Arpege) but different heat flux and wind stress forcing (respectively Arpege and ECMWF analyses). The Arpege wind and heat flux forcing lack of high frequency variability (compared to ECMWF analyses or data). The H2 experiment results into a deep top of the thermocline in the WP, while experiment H1 displayed a shallow one (compared to XBT data) (Maes, 1996). This results into a thicker BL in experiment H2. The underestimation of high frequency wind forcing partly explains the weak BLT values of our control experiment and suggests that the wind stress and the heat fluxes play a role in determining the BL depth. This is confirmed by experiment A5 , involving all the LMD forcings, where the easterlies are strong all over the Pacific. BLT in the WP is indeed very weak in this simulation, whereas it is increased when using the LMD water flux only and other Arpege forcing. The sensitivity of BL processes to the prescription of the water flux is tested in experiment A4, by using the surface water flux from the LMD AGCM, and the other forcing from Arpege. Figure 7 displays the BL average and its variance for experiment A4. The LMD water flux (see figure 4a) is globally stronger (and closer to the observations) and results in thicker BLs, especially under the ITCZ. The fact that BL comparable to AM composites appear under the ITCZ in experiment A4 and not in the C experiment suggests that direct freshwater forcing plays an important role in this region. In the warm pool and under the SPCZ, the stronger precipitations of the A4 experiment also result into thicker BLs, but to a lesser extent. This might be another clue to the thin BLs of the control experiment in this region. A new patch of thick BLs appears south of the equator, near 150°W in experiment A4. It is the result of a BL formation mechanism which is described in the second part of this paper, and that also appears (but not so clearly) in our control experiment. Finally, the LMD water flux displays a higher frequency and smaller spatial scale structure than the Arpege field. This is reflected by the BLT in the WP, more variable in experiment A4 via the halocline variability. Whereas the large scale variability of the BLT seems to depend on the upper current structure (see part II), its small

scale and high frequency variability in the WP is associated, at least partially, with the precipitation fields.

Let us also recall that the diurnal cycle had nearly no effect on the modeled BL (experiment A6). This means certainly that the large scale process of BL formation is not influenced by the diurnal cycle. This does not exclude that other smaller scale BL formation processes we do not simulate might be connected to this diurnal cycle.

We showed in part 3.1 that the simulated circulation and the thermohaline structure agree qualitatively with observed patterns. We just saw in the previous part that the main features of this haline structure were quite robust to the use of different forcing (A4, H1 and H2 experiments). This brings us some confidence in the processes that we have analyzed in the control experiment.

A.4.2. Vertical structure of the barrier layer and associated heat transport

The simulated profiles of temperature and salinity in the WP are often very similar to those observed by Lukas and Lindstrom (1991), or displayed in AM (see figure 8). In such cases, the top of the thermocline is much deeper than the top of the pycnocline, which is controlled by the haline stratification. A BL is present. Two questions arise from such a structure . Is the entrainment heat flux reduced because of the weakly thermally stratified bottom of the mixed layer? Is the net heat flux over this region very weak, in order to maintain the weak vertical temperature gradient between the surface mixed layer and the BL (Lukas and Lindstrom, 1991)? A mixed layer budget method (described in Appendix A) allows us to compute the average temperature tendency terms over the time-varying mixed layer depth. They feature advection (in three directions), horizontal diffusion, heat forcing and entrainment. We can answer the two previous questions by computing the average budget of the surface layer over the situations in which a thick (> 10 meters) BL is present in a WP box of experiment C (table 2, this (150°E, 170°W, 6°S, 6°N) box is defined in a region where BL is often thick: see figure 6a).

The heat advection tendency terms are weak in the WP, as well as the horizontal eddy mixing of heat (e.g. the zonal advection has values around -1.1 W.m^{-2} against 12.8 W.m^{-2} in the equatorial central Pacific, vertical advection is

0.1 W.m^{-2} against -5.5 W.m^{-2} in the central equatorial Pacific). Horizontal advection and eddy mixing are weak because the temperature is nearly homogeneous in the warm pool region. Temperature is also weakly stratified at the bottom of the mixed layer due to the BL: vertical advection is also very small. Only the meridional advection averaged over the 6°N-6°S is significant (6 W.m^{-2}), reflecting the poleward heat transport of equatorial heat by the gyre systems. However, too much attention should not be given to advection terms averaged over a box including several current regimes. We are more interested in defining what vertical transfers of heat between the surface and subsurface layer (by atmospheric forcing, entrainment and vertical advection) are typical of BL situations. Two facts are intriguing when considering these vertical heat transport. One point is that the entrainment flux and vertical advection at the bottom of the mixed layer are positive (e.g. the surface is heated up by the subsurface). This is unusual in the tropical ocean, where the cooler water is supposed to lie below the warmer. The other point is that the atmospheric forcing results in a negative tendency for the mixed layer (around -6.5 W.m^{-2}) whereas the net surface heat flux is positive (around 13 W.m^{-2}).

The clue to both these points appears in the vertical structure of the ocean in presence of a BL. In many simulated BL situations, the temperature profile shows an inversion supported by salinity stratification (see figure 8). Such a feature is also found in the BL profile displayed in AM. In these cases, the water of the surface mixed layer is slightly cooler than the underlying BL (about 0.1°C). Oceanic data collected at the ORSTOM center of Noumea (Delcroix and Eldin, 1995) has been investigated to see whether such inversions are common in the ocean. A systematic search on 1512 CTD profiles from COARE region (defined by the oceanic area bounded by 10°N, 10°S and 140°E, 180°E) shows that 41 % of the profiles in which a BL is present (with an average value of 27 meters) display a significant temperature inversion below the mixed layer. Patches of low salinity with slightly reduced temperature have furthermore been observed in the COARE region (Tomczack, 1995). This suggests that the temperature inversions in the BL are not a model bias but an average characteristic of the stratification in the WP. The vertical scale of these inversions is about the vertical scale of the BL (27 meters in data and 20 meters in the

model) and can certainly not be attributed to water mass intrusions which are of a smaller (~ 1-10 m) vertical scale (McPhaden, 1985). These inversions can be easily understood by considering the vertical distribution of atmospheric forcing in the WP upper ocean. The net surface heat flux over the COARE area in our control experiment is between -10 and 20 $W.m^{-2}$ (with a 13 $W.m^{-2}$ mean) over the 1985-1994 period. This is in the range of climatological estimates, which give around 20 $W.m^{-2}$ into the warm pool (Oberhuber, 1988). This net heat flux includes an incoming Arpege solar heat flux of about 235 $W.m^{-2}$ which is distributed over the first 100 meters of ocean (Jerlov, 1968; Siegel et al., 1995) and a non solar heat loss. This heat loss stems mostly from latent and long wave heat fluxes at the ocean surface. It is redistributed by turbulent processes over the whole mixed layer. The resulting atmospheric forcing of the surface mixed layer is expressed in equation (9) of appendix A, where Q_S is the incoming solar heat flux and $Q_S f(-h)$ is the fraction of this flux leaving the mixed layer. If this fraction is larger than the net heat flux, the overall effect of atmospheric forcing is to cool the mixed layer. That is what explains the negative value of atmospheric forcing of the mixed layer in the table 2, whereas the net heat flux is positive. The explanation of the positive entrainment terms follows naturally. Under the average condition of heat forcing encountered in the WP, the surface layer of the model has a tendency to cool. The underlying layer is below the effects of surface mixing: it does not feel the effect of the cooling surface flux Q^* but gets some heat from penetrative solar heat flux. Under the frequent rain conditions encountered in the WP, this differential heating (described in more details in appendix B) favors the development of temperature inversions. This situation leads to a positive entrainment of 2.5 $W.m^{-2}$ (table 2) over the BL regions in our control experiment. It can include both eddy mixing of mixed layer water with subsurface warmer water and convective overturning when salinity stratification is not strong enough to stabilize the inversion.

Some observations and other model studies depict similar processes. Convective overturning in fresh water lenses has been monitored during the COARE Intensive Observing Period (IOP) by Tomczack (1995). Cooling of the surface mixed layer, in presence of positive net heat flux and entrainment are depicted by Anderson et al. (1996) in the same region. Schneider et al. (1996) describe a similar effect of penetrative heat flux

in a CGCM (Coupled General Circulation Model). This brings us some confidence in the model results. However, Arpege solar heat flux is 40 $W.m^{-2}$ stronger than average annual estimates (see part 2.2.b). This results certainly in a slight overestimation of the differential heating in the control experiment (as it can be noted from equation (11) of appendix B). We have thus applied equation (11) to average annual heat flux data to verify that the penetrative solar heat flux might be responsible of the development of an inversion under the thin mixed layer conditions present in the WP. The average annual solar heat flux in the WP is around 195 $W.m^{-2}$ (Lewis et al., 1990). Several studies suggest that the net surface heat flux into the WP is around 20 $W.m^{-2}$ (e.g. Oberhuber, 1988), Q^* thus being close to -175 $W.m^{-2}$. Several studies using local estimates however suggest that this net surface heat flux is near zero, Q^* thus being close to -195 $W.m^{-2}$ (Lukas and Lindstrom, 1991; Godfrey and Lindstrom, 1989; Godfrey and al., 1991). We have used both these values of Q^* in our computations summarized in figure 9. A 40 meter average mixed layer depth of the equatorial WP ocean was used (Delcroix et al., 1992; AM). The result is a -0.15°C.$month^{-1}$ differential cooling with climatological values and -0.48°C.$month^{-1}$ when following a zero surface heat flux hypothesis. In both cases, the surface fluxes have a tendency to create a temperature inversion stabilized by haline stratification. The -0.48°C.$month^{-1}$ value (equivalent to a 30 $W.m^{-2}$ heat flux) seems too strong to be compensated by other fluxes in the warm pool region, where advection is weak and where low winds and thin mixed layer exclude a strong vertical mixing. The zero heat flux hypothesis is thus not necessary to explain the BL upholding in presence of a slightly positive net heat flux. The penetrative solar heat flux indeed leads to a slight cooling of the thin mixed layer and slight warming of the BL. Entrainment stemming from convective activity and wind stirring brings some heat back in the surface layer. This allows the surface layer to keep nearly the same temperature than the underlying layer.

The previous argument is based on long term average of the heat fluxes and mixed layer depth. These quantities have a strong variability over various time scales, including the diurnal cycle. We however think that our argument holds for seasonal to interannual timescales.

With the previous values of Q^* (Q^*=-175 W.m^{-2}), we can compute the minimum net heat flux that would heat up the surface layer by 0.5 °C more than the underlying layer, thus destroying the BL (see Appendix B). The result is 72 W.m^{-2} during one month, 57 W.m^{-2} during three months or 37 W.m^{-2} during one year. The BL can thus resist to long periods of positive net heat flux. Observations and 1D model results (Anderson et al., 1996) including the diurnal cycle support the role of penetrative solar heat flux in creating temperature inversions. These inversions are also present in experiment A6, suggesting that the previously described heat budget is also valid when including the diurnal cycle. Several studies however suggest that the mixed layer heat budget should display hysteresis in relation to the diurnal cycle. Rain events at specific hours of the day may for instance interact non linearly with mixed layer depth (Josse, 1996), nighttime mixing should be active at greater depth than the halocline (Anderson et al., 1996)... Only microstructure measurements and vertical heat budget sampling diurnal to interannual variability in the warm pool will learn us more about the role of the penetrative solar heat flux in the heat budget in this region.

A.4.3. Impact of the barrier layer on the surface layer heat budget

The previous section showed that the presence of BL could influence vertical heat transport by cutting off entrainment and vertical advection. We will now evaluate whether the variability of the BL is large enough to significantly modify the surface layer heat balance of the WP by cutting the entrainment cooling. Figure 10 displays the histogram of the entrainment as a function of the BLT, over the whole COARE region, and over a 170°E - 180°E, 2°N - 2°S region. In both regions, the entrainment flux is correlated with the BLT. There is a significant difference between oceanic situations without a BL (with an average entrainment heat flux of -18 W.m^{-2} in the equatorial box) and situations with a thin (10 meters = 1 model level) BL (with an average entrainment near zero). Further increase of the BLT is associated with an increasing positive entrainment. This increase of positive entrainment with increasing BLT (greater than 10 meters) happens in the whole COARE box. Positive entrainment is thus a feature common to all BL situations, and not to equatorial situations only.

The values of entrainment without a BL reach -18 W.m^{-2} in the equatorial region, whereas they do not exceed -5 W.m^{-2} over the whole COARE box. This might be explained by the strong shear turbulence in the equatorial region, compared to extra equatorial latitudes. In equatorial regions, zonal acceleration is directly forced by the wind momentum penetration, which is very sensitive to the stratification. This results in a strong and variable vertical shear. The mixed layer depth displays high frequency variations at the equator, associated with a strong variable entrainment. The entrainment flux is thus more strongly dependent on the BL absence / presence at the equator than at higher latitudes. The BLT variability near the equator should thus be studied with care.

A way to assess the role of haline stratification in the heat budget of the warm pool is to use sensitivity experiments where the salinity effects in the vertical mixing are switched off (experiment A1). Let us discuss the differences between the simulated SST of experiments C and A1. The 28°C and 29°C isotherm are shifted west by about 275 kilometers in A1 where the warm pool is colder. This can be partly attributed to increased westward currents near the dateline (see part 3.3) associated with upwelling and increased westward advection of central Pacific water (< 27 °C). This can also be linked to increased entrainment in A1 in the WP. Let us remind that the surface flux formulation for both C and A1 experiments includes a damping toward observed SST. It is thus difficult to fully evaluate the impact of the haline stratification on the SST in these experiments. We thus conducted two supplementary experiments, in which we switched off the heat flux feedback term in the WP. In A2 and A3 experiments, γ (see 2.2.b) is set to 0 inside the 140°E - 180°, 15°S - 15°N box, and smoothly interpolated to -40 W.m^{-2}.°C^{-1} within 5° of the borders of this area. Experiment A3 has no salinity effects in vertical mixing computations (see table 1). The main impact of cutting out the damping term is an increased SST variability. The model response to atmospheric forcing is stronger. For example, SST around 150°E dramatically decreases after a wind burst in February 86 in experiments A2 and A3, whereas the feedback term kept SST near observed values in the standard case. The increased variability leads to biases with the observed values up to 1.5°C. However, the general structure of the warm pool is not

affected (homogeneous temperature, longitudinal displacements, etc...). The model SST is now very different in A2 and A3. Average SST (for the year 1986 in figure 11) is globally colder in A3 in the western tropical Pacific (with differences up to 0.5°C near the equator at the dateline). This supports the idea that the haline stratification has a braking effect over the entrainment cooling of the surface layer. This effect is stronger near the equator, as suggested above. More precisely, the colder SST in experiment A3 is the result of a competition between several processes. First, the increase of entrainment cooling, due to the fact that the mixed layer extends down to the top of the thermocline. Meanwhile, the surface heat fluxes are distributed over a different thickness. The deeper the mixed layer, the more it keeps the penetrative solar heat flux, and the less it will be sensitive to the surface cooling. This is certainly why A3 is in some places warmer than A2. These sensitivity experiments prove qualitatively the role of haline stratification in the vertical mixing of air-sea properties into the ocean. However, they are conducted without any atmospheric feedback over the WP. Therefore they cannot help to estimate the relative importance of salinity related processes in the onset of El Niño. The effect of the BL on entrainment might indeed be emphasized or damped by atmospheric feedbacks. A quantitative analysis of the role of salinity in the upper ocean budget of the WP might be conducted with a coupled ocean - atmosphere model.

A.5. Summary and discussion

Summary

A primitive equation medium resolution model of the tropical Pacific was run over the 1985-1994 decade to investigate the role of the haline structure in the physics of the warm pool. The control experiment is forced by the daily surface fluxes from the AMIP simulation of the Arpege AGCM. The only damping toward observed values in the 20°N-20°S band is a local restoring term toward Reynolds and Smith (1994) SST in the surface heat flux. The surface salinity and circulation of this experiment are compared with available data and with sensitivity experiments using other forcing. The simulated surface circulation of the control does compare well with the observations. The westward penetration of the SEC is shown to be clearly related to the intensity and westward penetration of the easterlies. The general structure of the fresh and salty water mean

distribution are reproduced by the control experiment, but several strong (up to 1 psu) biases appear. The extreme sensitivity of the simulated SSS to the freshwater forcing suggests that most of these biases could originate from its structures.

Three regions of thick (10 to 15 meters) BL are robust in the model results. Two of them are located near the dateline: one near the equator and one in the 3°S - 8°S band. They correspond to regions of somewhat thicker (20 to 30 meters) BL in AM. The last thick BLT region appears around 120° West, 11° South and cannot be validated because of the lack of data in this area. The BLT over the whole Pacific ocean is shown to be very sensitive to the prescription of the water flux. The use of a more realistic water forcing (experiment A4) improves the BLT estimation, especially under the ITCZ where the local freshwater forcing might play an important role in the BL formation process.

The investigation of the vertical structure of the warm pool gives an insight of the vertical heat budget in this region. An inversion of the temperature profile sustained by haline stratification is often found in the BL in both model and COARE data. Following other studies (Siegel et al., 1995; Anderson et al., 1996; Schneider et al., 1996), we suggest that these inversions might be an average characteristic of the WP, caused by the interplay of thin mixed layers and strong solar heating. In these thin mixed layer regions of the WP, a significant part of the solar heating is lost beneath the surface layer. Simple calculations using both model and climatological values of the surface fluxes and mixed layer depth suggest that the underlying BL might heat up at a quicker rate than the surface layer (or might heat up while the surface layer cools). This vertical distribution of the atmospheric fluxes thus lead to the growth of an inversion sustained by haline stratification. This stratification is associated to positive entrainment fluxes at the bottom of the mixed layer (mixing with deeper warmer water) which could explain how a BL can persist over long time periods in presence of a positive net heat flux.

The impact of the BL on the surface layer budget is then analyzed. Both sensitivity experiments and a budget method lead to the following conclusions. The haline stratification acts as a barrier against entrainment cooling of the surface layer and even switches entrainment heating on for thick BLT. The entrainment difference with or without a BL is significant enough to modify the surface layer temperature by about 0.5°C, especially near the equator. On

the opposite, thick BLs are often associated to very thin mixed layers, which retain only a reduced part of the incoming solar heat fluxes thus diminishing SST heating rate. We thus suggest that BLs should act to "uncouple" ocean and atmosphere by inhibiting both entrainment cooling and solar heating of the surface layer. The haline stratification also inhibits downward penetration of turbulent kinetic energy in the WP ocean. This results in a trapping of WWB momentum in the surface layer of the fresh pool, giving rise to strong fresh equatorial jets. In relation with the large scale convergence hypothesis of Picaut et al. (1996), we thus suggest that the salinity might have an active role in the setting of the eastern edge of the warm and fresh pool.

Discussion

The modeling framework and the use of AGCM daily forcing are the source of several uncertainties in this study. First, the horizontal (about 100 km) and vertical (10 m) resolution of the model might not be sufficient in comparison with the horizontal and vertical structures associated to haline effects in this region. The use of daily forcing (wiping out the diurnal cycle) can also appear insufficient. Sensitivity tests with higher resolution give very similar results, as well as test with an idealized daily cycle. This might be partly because of the poor (275 kilometers) resolution of atmospheric fluxes which do not force the growth of small scale oceanic structures. This also indicates that at least one part of BL formation and variability is related to rather large scale and low frequency processes. Some fine scale structures (Tomczack et al, 1996; You, 1995) can however not be accounted for by the OGCM. These small scale formation processes could contribute to the large scale BL structure. Further regional modeling in the COARE region might teach us more about these scale interactions. Moreover, a recent study has shown the impact of horizontal diffusion on the large scale simulated circulation in the model (Maes et al, 1996). The dynamics in the warm pool is obviously dependent on parameter choices in the model and more testing about mixing is needed.

Another source of uncertainty in this study is the simulated circulation and thermohaline structure. Given the sparse time-space coverage of salinity observations, evaluation of model results is hard. There is however a good large scale structure correspondence of simulated and observed SSS and BLT (AM). Several systematic biases still remain (low SSS, thin BLT) which might lead to a biased estimate of the effects of haline stratification. The simulated SSS in the WP is indeed too low. The subsurface salinity being correctly simulated, the vertical haline stratification is overestimated in the WP. This might lead to an overestimation of haline stratification effects. On the opposite, the BLT is underestimated. It is difficult to say how these opposite effects compensate.

Let us suggest some conclusions from this study.

Cooper [1988] already highlighted the importance of the salinity field in dynamic height computations in the tropical Pacific. We have furthermore shown the importance of haline stratification in the wind driven dynamics of the upper layer of the fresh pool. Salinity also plays a role in the upper ocean heat budget. We strongly suggest that numerical studies of air sea interaction covering the WP should include a salinity prognostic equation.

Our results suggest that the haline structure can significantly modify the surface layer heat budget and dynamical response. It is thus important to understand which processes govern BL formation and variability. The part II of this paper investigate the large scale formation mechanisms in the model. It also describes their response to the interannual variability.

Finally, the "forced" framework is a strong limit in this study. To fully estimate the BL impact on the upper ocean heat budget, the whole air sea interaction loop has to be accounted for. We will continue the study in a coupled framework, in order to validate the effect of the BL upon the SST.

A. References

Anderson, S.P., R. A. Weller and R.B. Weller, 1996, Surface buoyancy forcing and the mixed layer of the western Pacific warm pool: observations and 1-D model results, *J. Clim.*, in press.

Ando, K. and McPhaden, M.J., 1997, Variability of surface layer hydrography in the tropical Pacific ocean, submitted to *J. Geophys. Res.*

Arakawa, A., 1972, Design of the UCLA general circulation model. Numerical simulation of weather and climate, *Rep. Tech. Report 7*, Dept. of Meteorology, University of California.

Arkin, P.A. and P.E. Ardanuy, 1989, Estimating climatic - scale precipitation from space: a review. *J.Climate*, 115, 51-74.

Asselin, R., 1972, Frequency filter for time integration, *Mon. Wea. Rev.*, 100, 487-490.

Blanke, B. and P. Delecluse, 1993, Variability of the tropical Atlantic ocean simulated by a general circulation model with two different mixed layer physics, *J. Phys. Oceanogr.*, 23, 1363-1388.

Chen, D. and L. M. Rohstein, 1991, Modeling the surface mixed layer structure in the western equatorial Pacific, unpublished manuscript (*TOGA notes*, 2, 13-16).

Cooper,N.S., 1988, The effect of salinity on tropical ocean models, *J. Phys. Oceanogr.*, 18, 697-707.

Dandin, P., 1993, *Variabilité basse fréquence simulée dans l'ocean Pacifique tropical*, Thèse de doctorat de l'université Pierre et Marie Curie.

Delcroix, T., G. Eldin, M.-H. Radenac, J. Toole and E. Firing, 1992, Variation of the western equatorial Pacific Ocean, 1986-1988. *J. Geophys. Res.*,96 (suppl.), 3249-3262.

Delcroix, T., G. Eldin, 1995, Observations hydrologiques dans l'océan Pacifique tropical ouest, TDM 141, ORSTOM Ed., 77 pp.

Delcroix, T., C. Henin, V. Porte and P. Arkin, 1996, Precipitation and Sea - Surface Salinity in the Tropical Pacific, 1974 - 1989, *Deep Sea Res.*, in press.

Delcroix, T., J. Picaut, 1997, Zonal displacement of the western equatorial pacific fresh pool, submitted to *J. Geophys. Res.*

Delecluse, P., G. Madec, M. Imbard and C. Lévy, 1993, OPA version 7 General Circulation Model reference manual, LODYC, France, internal report 93/05.

Déqué, M., C. Dreveton, A. Braun and D. Cariolle, 1994, The ARPEGE/IFS atmosphere model : a contribution to the french community climate modelling, *Climate Dyn.*, 10, 249-266.

Déqué, M., 1995, Sensitivity of the Météo-France/CNRM GCM to horizontal resolution, Proceedings of the first international AMIP scientific conference, *WMO/TD-No. 732*.

Godfrey, J.S. and E. Lindstrom, 1989, On the heat budget of the equatorial west Pacific surface mixed layer, *J. Geophys. Res.*,94, 8007-8017.

Godfrey, J.S., M. Nunez, E.F. Bradley, P.A. Coppin and E.J. Lindstrom, 1991: On the net surface heat flux into the western equatorial Pacific, *J. Geophys. Res.*, 96 (suppl), 3391 - 3400.

Hellermann, S. and M. Rosenstein, 1983, Normal monthly wind stress over the world ocean with error estimates, *J. Phys. Oceanogr.*, 13, 1093-1104.

Jerlov, N. G., 1968,*Optical Oceanography*, 194 pp., Elsevier.

Levitus, S., 1982, Climatological atlas of the world ocean, *Rep.NOAA Prof. Paper 13*, NOAA.

Lewis, M.R., M.E. Carr, G.C. Feldman, W. Esaias and C. McClain, 1990, Influence of penetrating solar radiation on the heat budget of the Equatorial Pacific Ocean, *Nature*, 347, 543-545

Lukas, R., 1988, On the role of western Pacific air-sea interaction in the El Niño / Southern Oscillation phenomenon. *Proceedings of the U.S. TOGA Western Pacific Air Sea Interaction Workshop*, Honolulu, 16-18 September, 1987. R. Lukas and P. Webster, U.S. TOGA Rept. USTOGA-8, 43-69.

Lukas, R. and E. Lindström, 1991, The mixed layer of the western equatorial Pacific ocean, *J. Geophys. Res.*, 96, 3343-3457.

Maes, C., G. Madec and P. Delecluse, 1997, Sensitivity of an equatorial Pacific OGCM to the lateral diffusion, *Monthly Weather Review*, in press.

Maes, C, 1996, Equilibre du reservoir chaud de l'océan Pacifique tropical ouest, Thèse de doctorat de l'université Pierre et Marie Curie, 255pp.

McPhaden, M.J., 1985, Fine-structure variability observed in CTD measurements from the central equatorial Pacific, *J. Geophys. Res.*, 90, 11726-11740.

McPhaden, M.J., F. Bahr, Y. Dupenhoat, E. Firing, S.P. Hayes, P. Niiler, P.L. Richardson and J.M. Toole, 1992, The Response of the Western Pacific Ocean to Westerly Wind Bursts During November 89 to January 90, *Journal of Geophys. Res.*, Vol 97, No C9, 14289 - 14303.

Miller, J., 1976, The salinity effect in a mixed layer ocean model, *J. Phys. Oceanogr.*, 6, 29-35.

Millero, F. S. and A. Poisson, 1981, An international one-atmosphere equation of state of sea-water, *Deep-Sea Res.*, 28A, 625-629.

Oberhuber, J. M., 1988, An atlas based on the COADS data set: the budgets of heat, buoyancy and turbulent kinetic energy at the surface of the global ocean, *Report No 15 Max Planck Institut fur Meteorologie*, 20 pp.

Picaut, J., M. Ioulalen, T. Delcroix, M. J. McPhaden and C. Menkes, 1996, Mechanism of the zonal displacements of the Pacific warm pool: implications for ENSO, *Science*, 274, 1486 - 1489.

Reverdin, G., C. Frankignoul, E. Kestenare and M.J. McPhaden, 1994, Seasonal variability in the surface currents of the equatorial Pacific, *J. Geophys. Res.*, 99, 20323 - 20344.

Reynolds, R. W., 1988, A real time global sea surface temperature analysis, *J. Climate, 1*, 3283-3287.

Sadourny, R. and K. Laval, 1984, January and july performance of the LMD general circulation model, *New perspectives in climate modelling*, A. Berger Ed., Elsevier, 173-198.

Shinoda, T. and R. Lukas, 1995, Lagrangian mixed layer modelling of the western equatorial Pacific, *J. Geophys. Res.*, 100, 2523-2541.

Schneider N., T. Barnett, M. Latif, T. Stockdale, 1996, Warm pool physics in a coupled GCM, *J. of climate*, 9, 219 - 239.

Siegel D.A., J.C. Ohlmann, L. Washburn, R. Bidigare, C.T. Nosse, E. Fields and Y. Zhou, 1995, Solar radiation, phytoplankton pigments and the radiant heating of the equatorial Pacific warm pool, *J. Geophys. Res.*, 100, 4885 - 4891.

Slingo, J.M., K.R. Sperber, J.S. Boyle, J.-P. Ceron, M. Dix, B. Dugas, W. Ebisuzaki, J. Fyfe, D. Gregory, J.-F. Gueremy, J. Hack, A. Harzallah, P. Inness, A. Kitoh, W.K.-M. Lau, B. McAvaney, R. Madden, A. Matthews, T.N.

Palmer, C.-K. Park, D. Randall, N. Renno, 1996. Intraseasonal oscillation in 15 atmospheric general circulation models: results from an AMIP diagnostic subproject. *Climate Dyn.*, 12, 325-357.

Spencer, R. W., 1993, Global oceanic precipitation from the MSU during 1979-91 and comparisons to other climatologies, *J. Climate*, 6, 1301 - 1326.

Sprintall, J. and M. J. McPhaden, 1994, Surface layer variations observed in multiyear time series measurements from the western equatorial Pacific, *J. Geophys. Res.*, 99, 963-979.

Sprintall, J. and M. Tomczak, 1992, Evidence of the barrier layer in the surface layer of the tropics, *J. Geophys. Res.*, 97, 7305-7316.

Tomczack, M., 1995, Salinity variability in the surface layer of the tropical western Pacific Ocean, *J. Geophys. Res.*, Vol. 100, 20499 - 20515.

Vialard and Delecluse, 1997b, An OGCM study for the TOGA decade. Part II: Barrier layer formation and variability, *J. Phys. Oceanogr.*, 1996.

You, Y., 1995, A rain formed barrier layer model, *Ocean modelling*, Issue 106, March 1995.

A. Appendix A: mixed layer heat budget method

As we are interested in the effect of BL presence on entrainment cooling of the surface layer, we develop a method to integrate the tracer equation over the simulated mixed layer. This method allows to get the different tendency terms governing the variability of the surface temperature and salinity: horizontal advection, horizontal diffusion, forcing and entrainment from below.

The equations of temperature is written in the model as follows (the equation for salinity being the same with different boundary condition, and without the penetrative heat flux term):

$$\partial_t T = -u\partial_x T - v\partial_y T - w\partial_z T + \partial_z(K_\rho \partial_z T) + Q_s \partial_z f(z) + D_h(T) \underset{=R}{}$$
(1)

with the following surface boundary condition:

$$(K_\rho \partial_z T)_{z=0} = Q^* / \rho_0 C_P$$
(2)

T is the potential temperature, K_ρ the vertical diffusion coefficient, D_h the horizontal diffusion operator, u the zonal current, v the meridional current, w the vertical current, $\rho_0 C_P$ the volumic specific heat of seawater, Q^* the non penetrative part of the surface heat flux, Q_s the penetrative solar heat flux. f(z) is the fraction of solar heat flux heating that reaches the depth z, f(z)=Rexp(z/l1)+(1-R)exp(z/l2) with R=0.58, l1=0.31m and l2=20m for a type I water (Jerlov, 1968).

The mixed layer depth h, over which the tracer equation is integrated, is computed using a density criterion: the bottom of the first model level where density is higher than the sea surface density plus 0.05 kg.m^{-3}. This value is chosen empirically to fit at best to the simulated mixing layer on a 1-3 day basis. (We define the model mixing layer as the layer in which the vertical mixing coefficient is higher than 5.10^{-4} m^2.s^{-1}. We did not use this layer to compute the surface heat/salt budget because it displays very high frequency variations to which the tracer profiles sometimes do not have time to adjust.)

Integrating (1) over the time - varying mixed layer depth, we get the classical integral mixed layer model equation:

$$\partial_t T = \frac{1}{h}\int_{-h}^{0} R dz + \frac{\partial_t h}{h}(T_{-h} - \overline{T})$$
(3)

where R stands for the right hand side of (1), $\overline{T}$ is the integrated temperature over the surface layer and T_{-h} the temperature at the bottom of this layer.

Equation (3) can be written as:

$$\partial_t \overline{T} = \overline{A}_x + \overline{A}_y + \overline{A}_z + \overline{D}_h + F + E$$
(4)

where:

$$\overline{A}_x = -\frac{1}{h}\int_{-h}^{0} u\partial_x T dz$$
(5) is the zonal advection over the whole layer. (We do not separate the horizontal entrainment of interior ocean water into a sloping mixed layer by horizontal advection from the total tendency term: we found it to be negligible.)

$$\overline{A}_y = -\frac{1}{h}\int_{-h}^{0} v\partial_y T dz$$
(6) is the meridional advection over the whole layer.

$$\overline{A}_z = -\frac{1}{h}\int_{-h}^{0} w\partial_z T dz = \frac{1}{h}\left(w_{-h}(T_{-h} - \overline{T}) + \int_{-h}^{0} (T - \overline{T})\partial_z w dz \right)$$
(7) is the vertical advection

over the whole layer. A_z is found to be nearly equal to $\frac{1}{h} w_{-h}(T_{-h} - \overline{T})$ and could be included in the entrainment tendency term (10).

$$\overline{D}_h = \frac{1}{h}\int_{-h}^{0} D_h dz$$
(8) is the effect of horizontal diffusion over the layer.

$$F = \frac{Q^* + Q_s(1 - f(-h))}{\rho_0 C_P \times h}$$
(9) is the combined effect of short-wave heating and surface cooling.

$$E = \frac{1}{h}\left(\partial_t h(T_{-h} - \overline{T}) + \frac{(K\partial_z T)_{-h}}{\rho_0 C_P}\right)$$

(10)   is the overall effect of underlying water on the surface layer. It features entrainment of water from below, turbulent flux into the surface layer.

This rearrangement of the equations is relatively easy when done using a analytical formulation. It is far more complicated with the discretized form of the equations used in OPA. This is because the Asselin (1972) filter mixes odd and even time steps. We have shown, using the discrete equations, that the term $e = \_t h(T_{-h} - \overline{T})/h$ could not be written otherwise than as the residual of the other terms from equation (3). This implies that this term will be known to an accuracy not better than the Asselin correction term. Still, this accuracy can be increased when considering the budget over a period of several time steps. Let us say that α is the Asselin coefficient and N the number of time steps over which we compute the budget. The error made on the entrainment term is ~ $2\alpha/N*\_t T$. When the entrainment is the dominant term of the budget (i.e. $e \sim \partial_t T$, the worse case for precision), we reach a accuracy of 0.25 % (we choose N=80 - 5 days - and α is 0.1). The second source of error in computing the entrainment as a residual from the other terms comes from the fact that the surface layer is not perfectly homogeneous in temperature or salinity. Still, this effect is negligible.

A. Appendix B: atmospheric forcing of the mixed layer

The net heat flux at the ocean atmosphere interface includes a penetrative solar heat flux Q_s and a non penetrative part Q^*. Q^* includes the sensible, latent and long-wave heat fluxes (and should also include the heat flux associated to rain events, which is not accounted for in our experiments). Q^* is almost always a heat loss at the ocean surface, distributed by turbulent processes over the whole mixed layer. Let us now compute the differential heat budget of the mixed layer and underlying layer, associated to the effects of surface forcing only.

For the surface mixed layer it is F as given by (9) of appendix A. For a b meters thick underlying BL, the heat gain associated to forcing is only due to solar heating:

$$F' = \frac{Q_s}{\rho_0 C_P b}(f(-h) - f(-h-b))$$

, supposing that interior mixing distributes the penetrative solar heat flux over the BLT. The differential heating between the surface layer and the subsurface layer is F-F'. The stratification S_a (temperature difference) created by the atmospheric fluxes over a time τ between the mixed layer and the underlying layer is expressed as:

$$\frac{S_a}{\tau} = \frac{1}{\rho_0 C_P}\left(\frac{Q^*}{h} + Q_s\left(\frac{1-f(-h)}{h} - \frac{f(-h) - f(-h-b)}{b}\right)\right)$$

(11)

- A positive value of S_a/τ corresponds to a stratification under the effect of solar heating. Using (11), it is easy to get the net heat flux value necessary over a time τ to create a S_a °C stratification between the h meters mixed layer and the underlying layer, for a given Q^* non solar heat flux:

$$Q_{net} = Q^* + \frac{\rho_0 C_P h \frac{S_a}{\tau} - Q^*}{1 - f(-h) - hb^{-1}(f(-h) - f(-h-b))}$$

(12)

- A negative value of S_a/τ results in a slower heating of the surface than of the subsurface. The temperature inversion that appears at the bottom of the mixed layer is first a source of positive *diffusive entrainment*: heating of the surface layer by eddy mixing with subsurface warmer water ($(K\partial_z T)_{-h} / (\rho_0 C_P h)$ term of equation (10)). If this positive diffusive entrainment compensates the effects of the cooling by the atmospheric fluxes, the mixed layer stays stable. If the cooling of the mixed layer is too strong (e.g. in the case of a negative net heat flux), convective overturning starts and mixed layer deepens until *convective entrainment* of deeper warmer water ($\partial_t h(T_{-h} - \overline{T}) / h$ term of equation (10)) stabilize the mixed layer.

FIGURES (*Annexe A*)
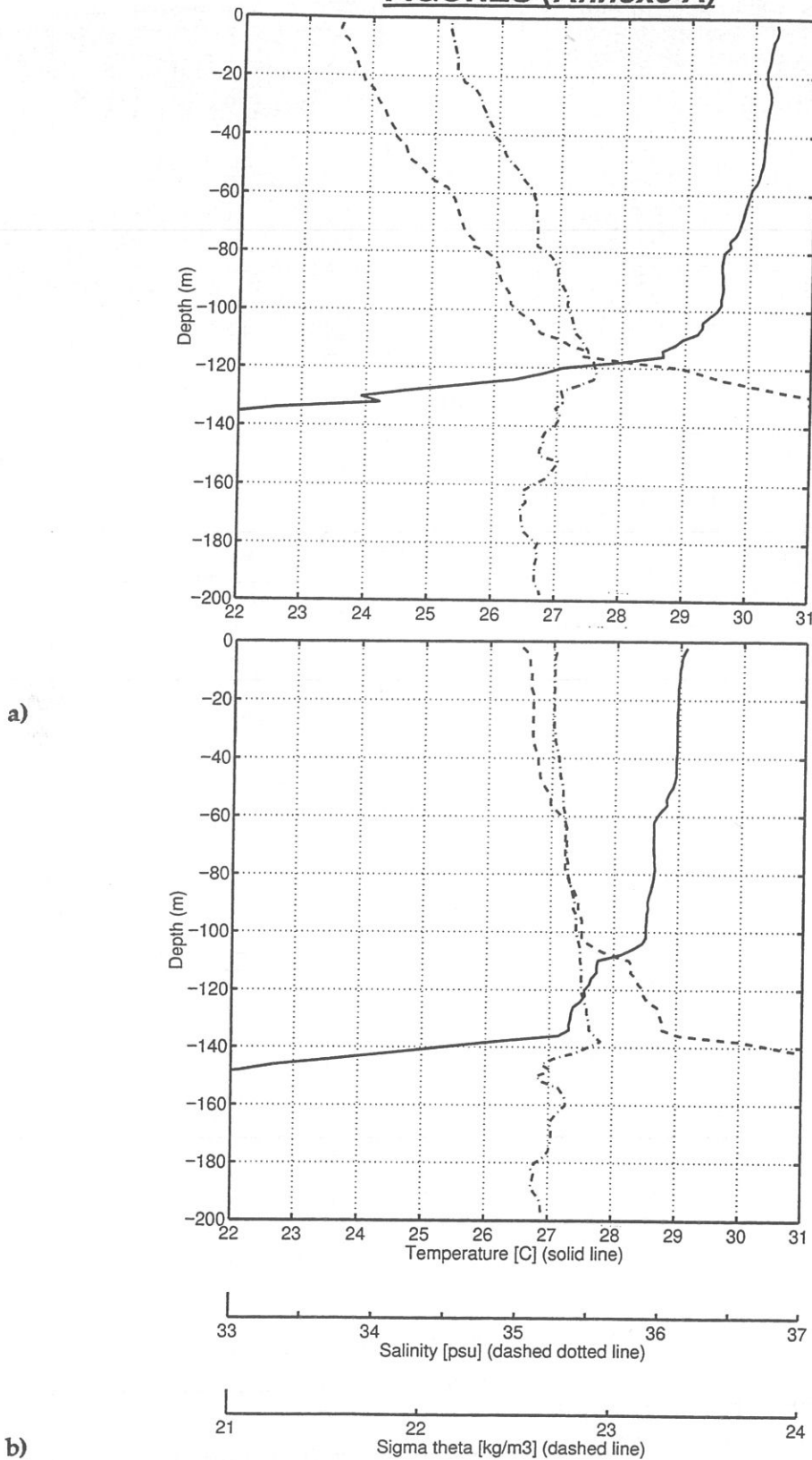
Figure A.1. Temperature, salinity and density profiles measured during the FLUPAC campaign, a) at 177.4 °West, b) at 155.4 °West. The top of the thermocline and bottom of the mixed layer computed from the (SST - 0.5°C) and (sea surface density + $\partial\rho/\partial T (SST, SSS)$*(-0.5°C)) criterions are given on profile a) where there is a thick BL.
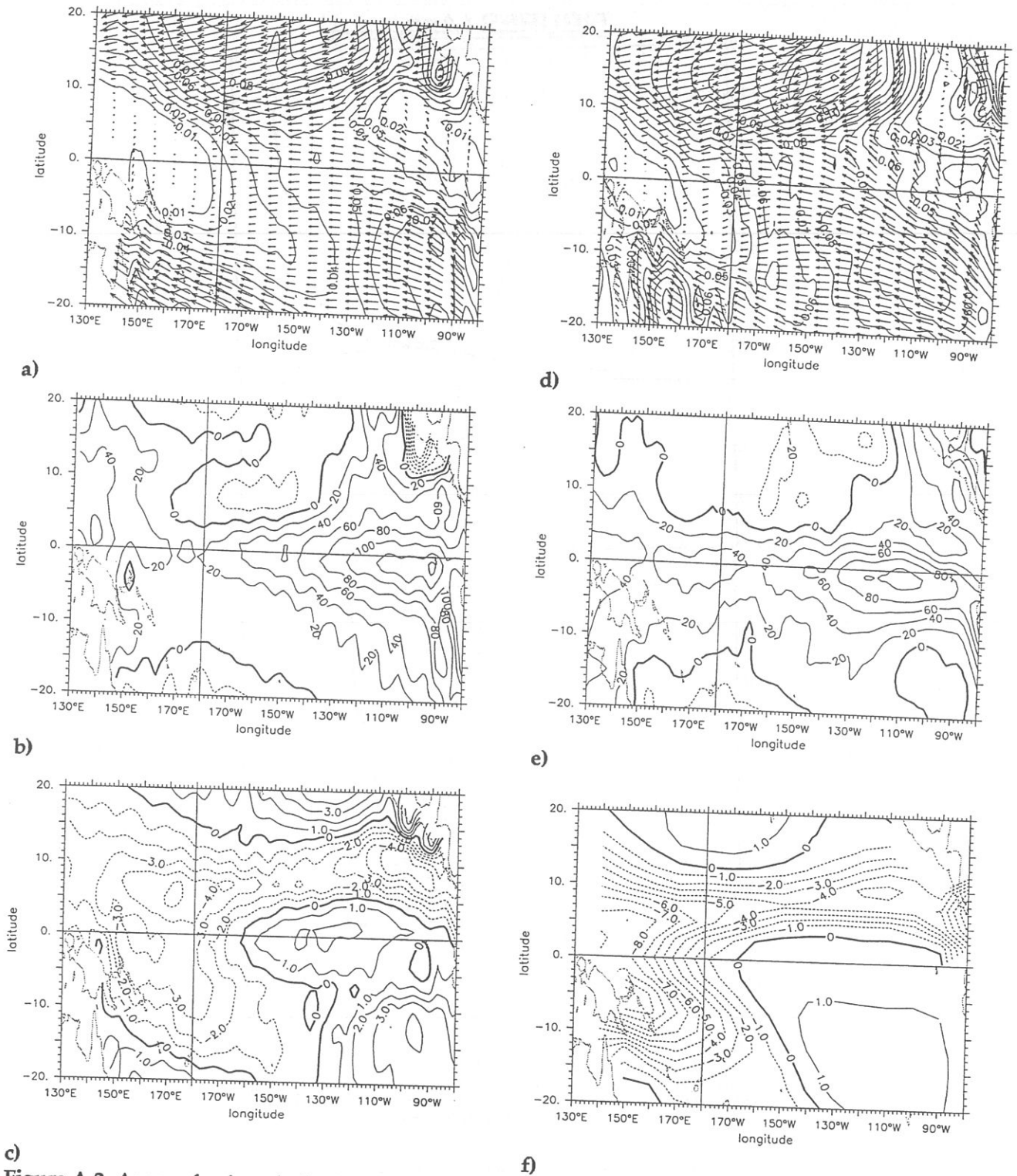
Figure A.2. Arpege forcings (a, b, c) and observed forcings (d, e, f) over the Pacific Ocean. a) and d) are the wind stresses in N.m^{-2}, with a 0.01 contour interval. b) and e) are the net heat fluxes in W.m^{-2}, with a 20 W.m^{-2} contour interval. c) and f) are the freshwater fluxes in mm.day^{-1}, with a 1 mm.day^{-1} contour interval. (d) is from Hellerman and Rosenstein (1983), (e) from Oberhuber (1988) and (f) from Arkin and Ardanuy (1989).
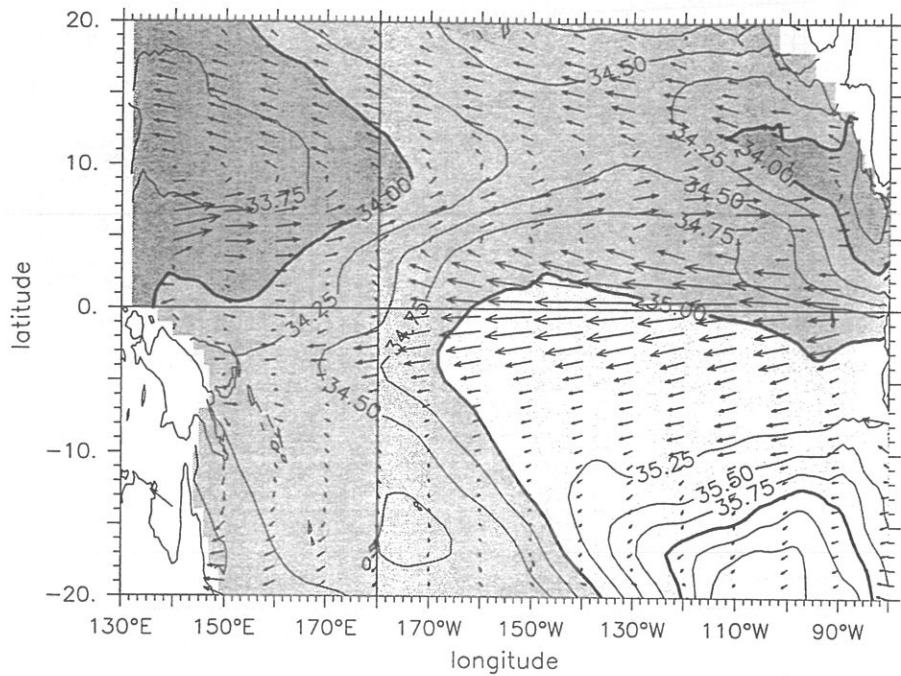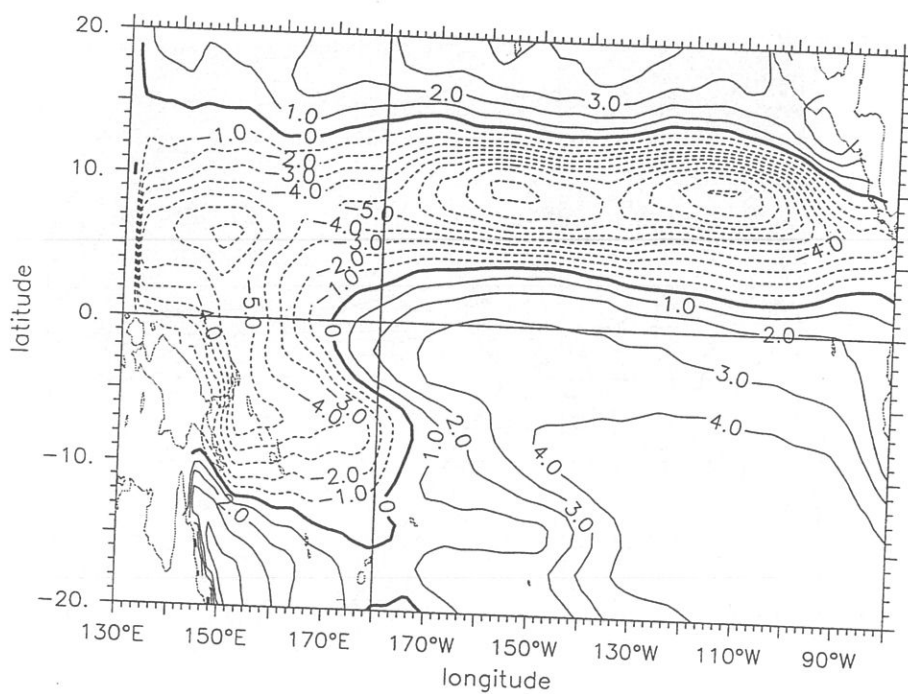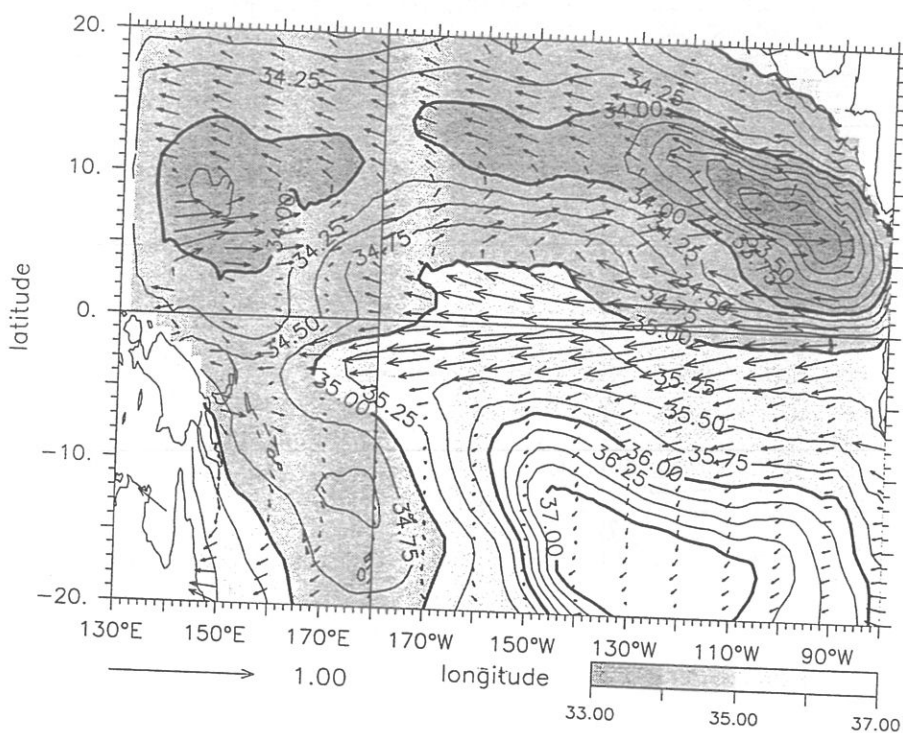
a)
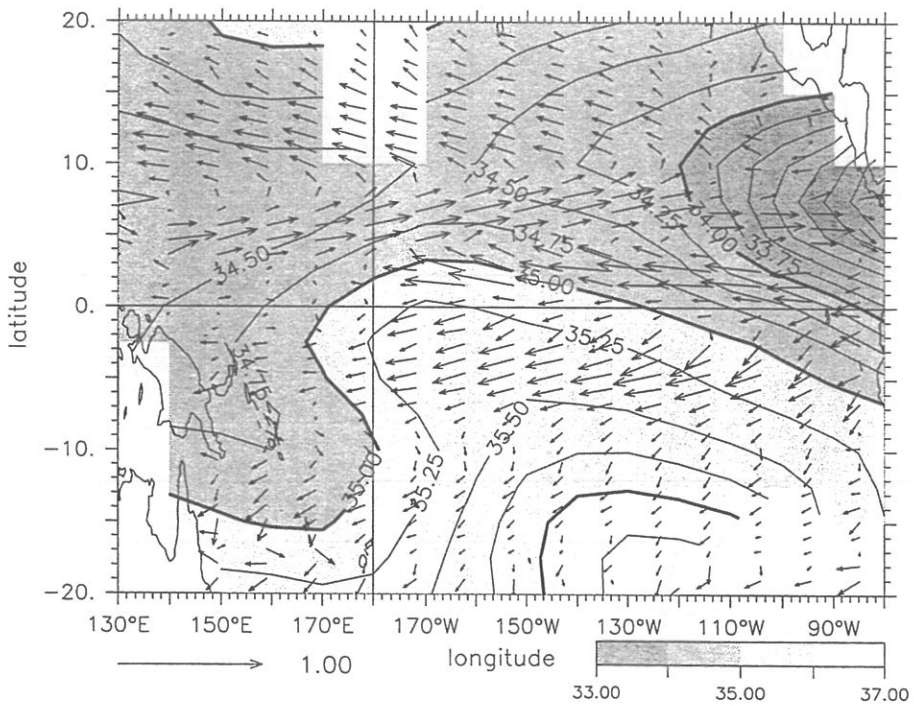
b)

Figure A.3. Sea surface salinity and surface current (a) From our control experiment. (b) From Delcroix *et al.*, (1996) and Reverdin *et al.* (1994) climatologies. Contour interval for SSS is 0.25 psu.
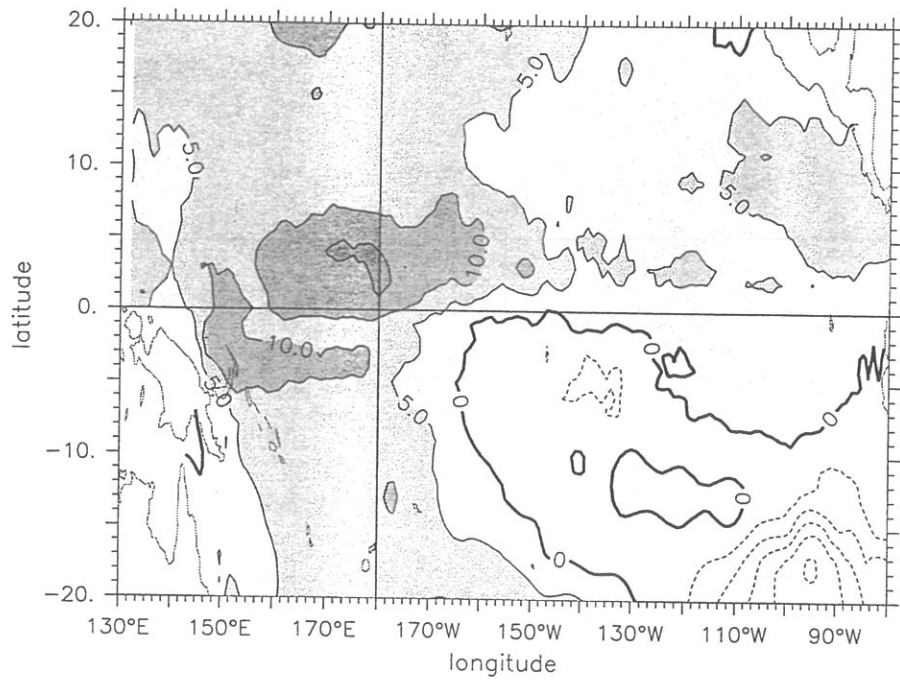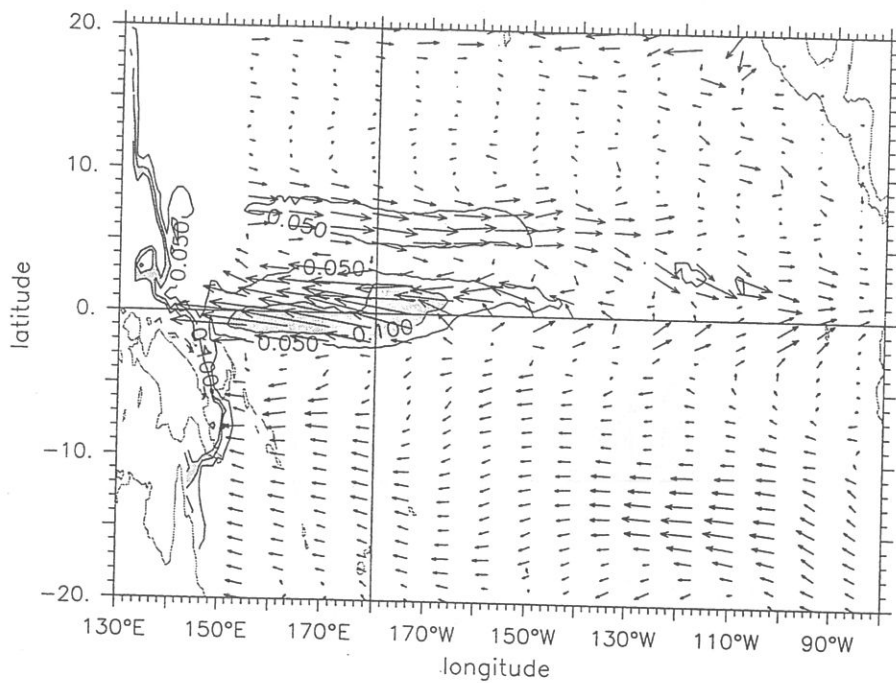
a)

b)

Figure A.4. (a) LMD freshwater flux averaged over 1985 - 1994, in mm.day^{-1}, with a 1 mm.day^{-1} contour interval. (b) Simulated SSS (experiment A4) in experiment A4, in psu with a 0.25 psu contour interval.
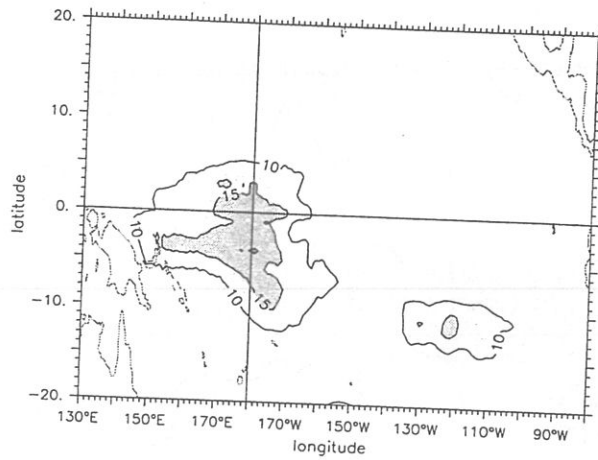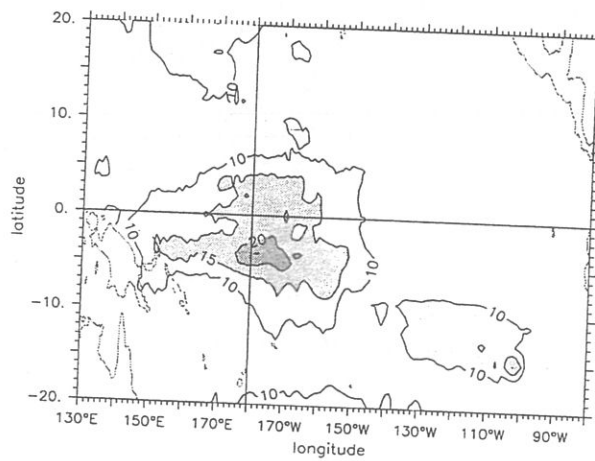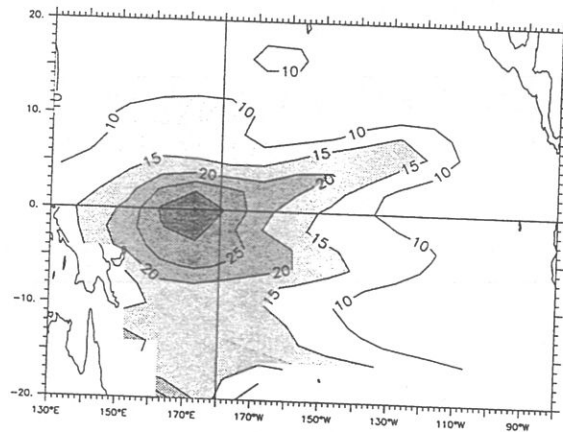
a)

b)

Figure A.5. A1 experiment (without salinity in vertical mixing) minus control experiment. (a) mixing layer depth, units in m, contour interval is 5 m, grey tones correspond to a deeper mixing layer in the A1 experiment. (b) surface currents, units in m.s^{-1}, with a 5 cm.s^{-1} contour interval and differences greater than 5 cm.s^{-1} in grey tones.
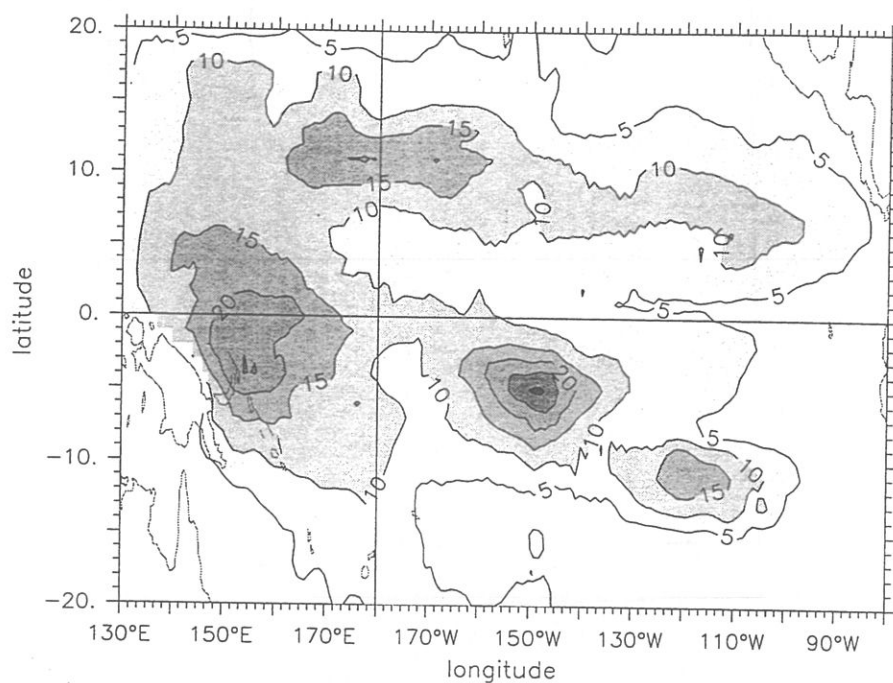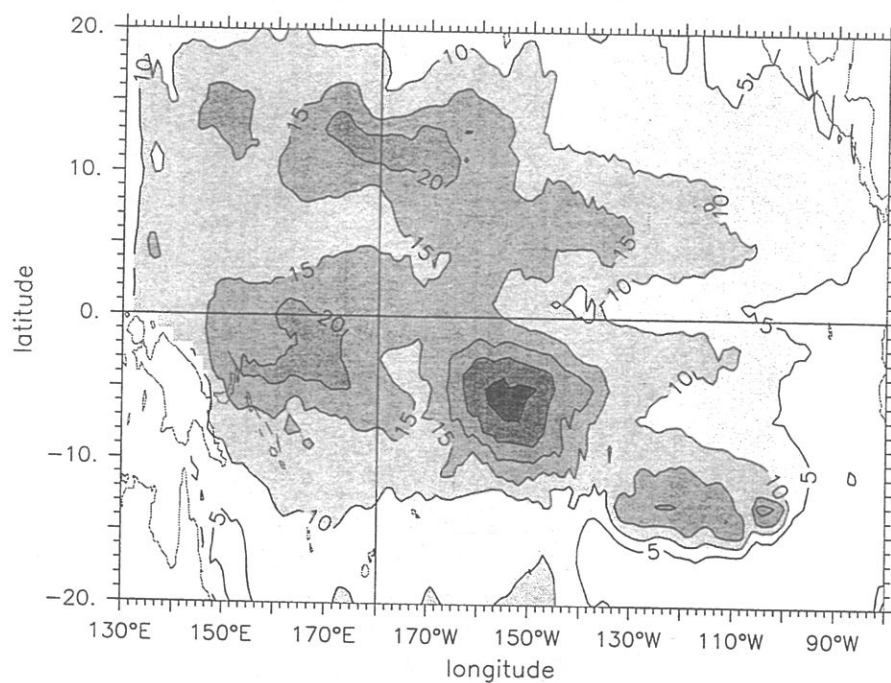
a)

b)

c)

Figure A.6. (a) Simulated BLT of the control experiment (b) and its variance (from 5 days averages). (c) BLT composite for normal years from AM. Units are in meters. Contour interval is 5m.
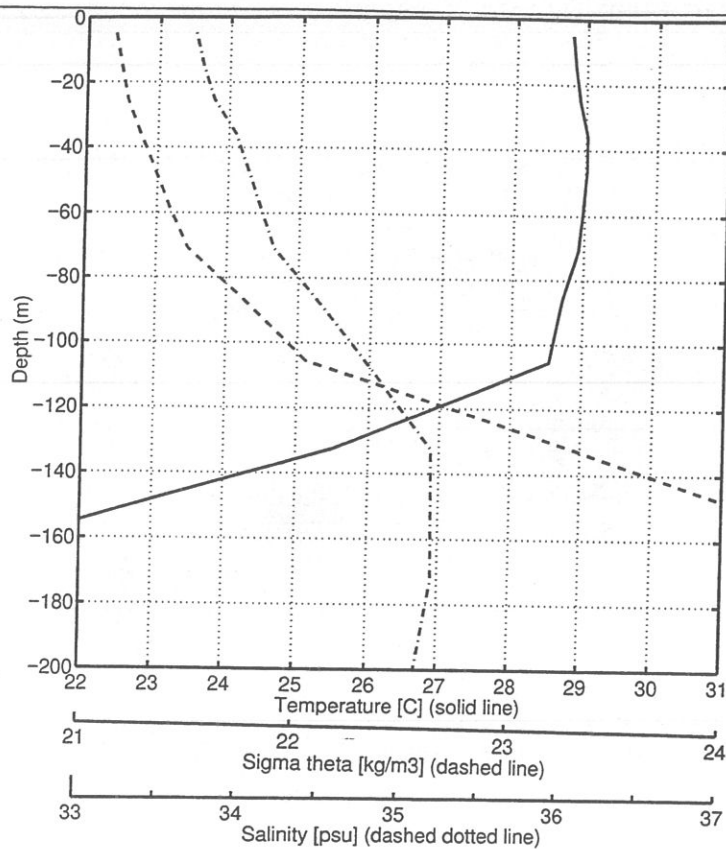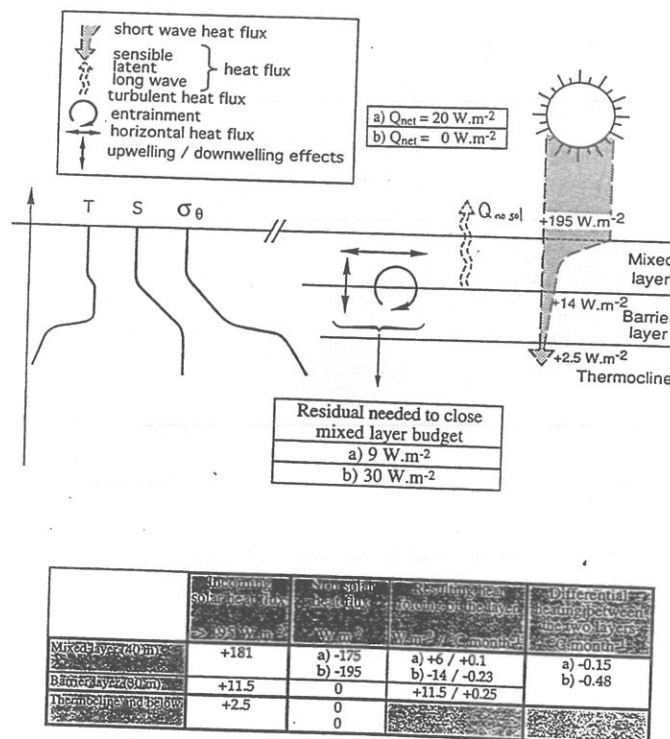
a)

b)

Figure A.7. (a) Simulated BLT of experiment A4 (b) and its variance (from 5 days averages). Units are in meters. Contour interval is 5m.

Figure A.8. Monthly mean temperature, salinity and potential density simulated profiles in a situation where BL is present. Top of the pycnocline and top of the thermocline are marked by horizontal lines, according to Sprintall and Tomczack (1992) criterion.

	Incoming Solar heat flux > 195 W.m-2	Non solar heat flux W.m-2	Resulting heat forcing on the layer W.m-2 / °C.month-1	Differential heating between the two layers °C.month-1
Mixed layer (40 m)	+181	a) -175 / b) -195	a) +6 / +0.1 / b) -14 / -0.23	a) -0.15 / b) -0.48
Barrier layer (80 m)	+11.5	0	+11.5 / +0.25	
Thermocline and below	+2.5	0 / 0		

Figure A.9. Simplified vertical heat budget in presence of BL in the warm pool region. The table recapitulates the budget of the mixed layer and BL. Two hypotheses for the outgoing radiative heat flux have been selected: (a) following the climatologies, (b) following the zero net heat flux hypothesis. The fluxes arising from horizontal processes and entrainment needed to maintain a zero heating in the mixed layer are computed as the residual of the forcing terms.
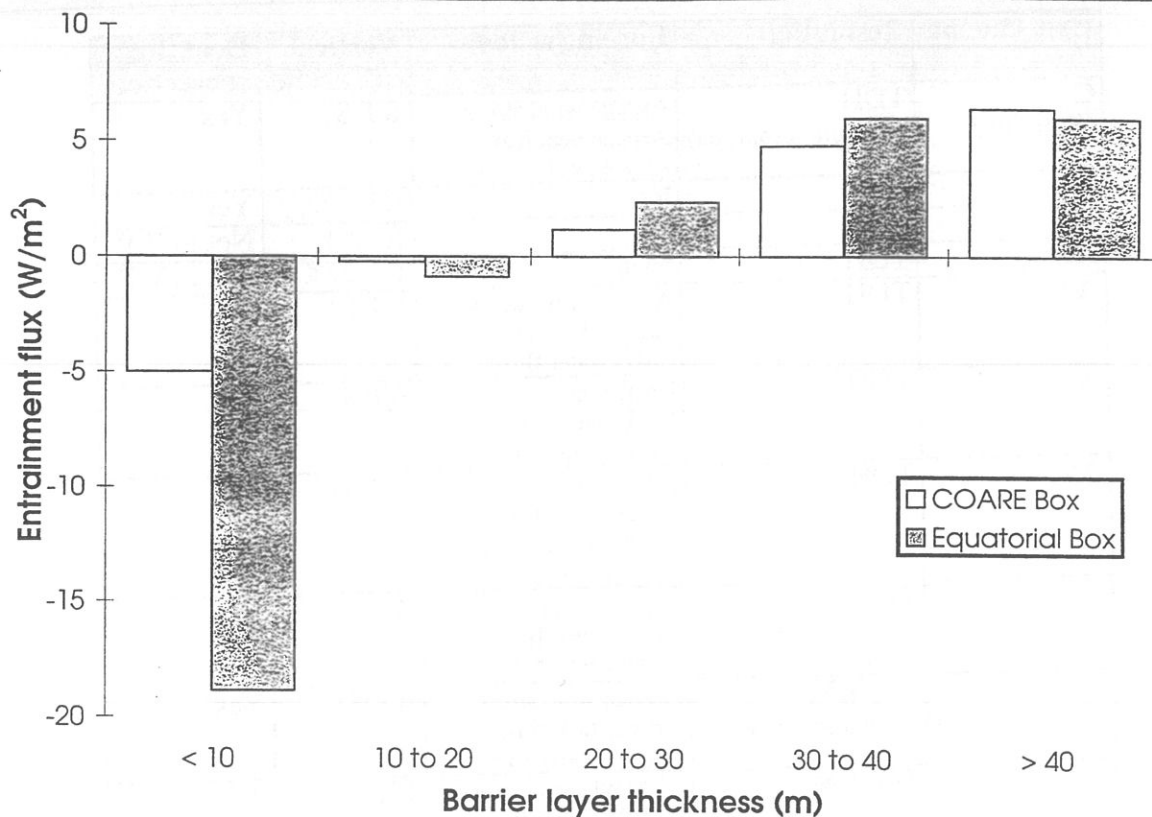
Figure A.10. Histogram of entrainment flux at the bottom of the mixed layer against the 5 day averaged BLT of our control experiment. Values averaged over the COARE (10°N-10°S, 140°E-180°E) box are in black. Values averaged over the 170°E - 180°E, 2°S - 2°N box are in white. Units are in $W.m^{-2}$. 5 day averaged values of BLT less than 10 m mean that there was no BLT on the average, between 10 and 20 m means that there was a 1 to 2 model levels BLT on the average, etc...
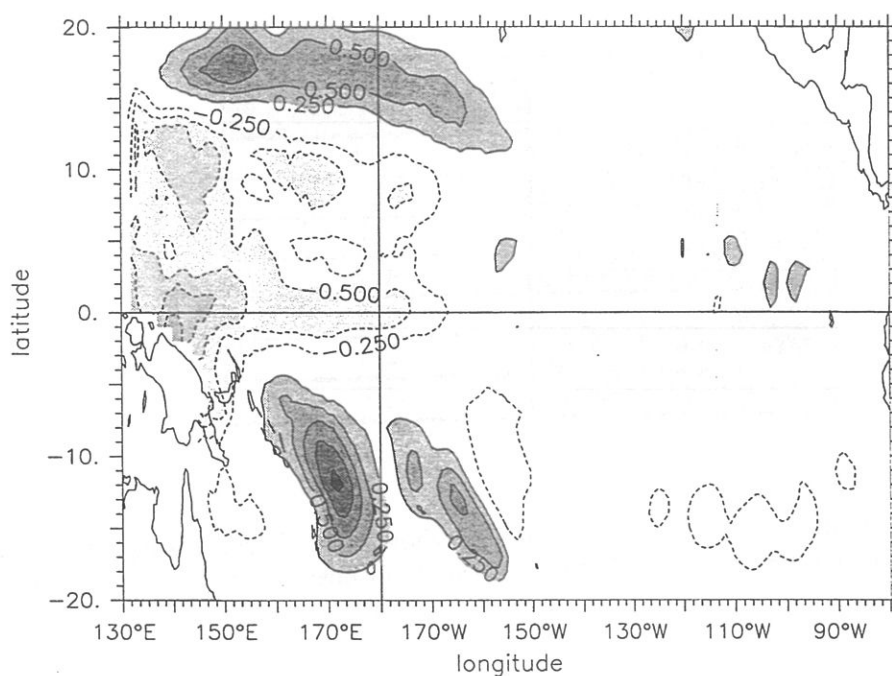
Figure A.11. SST difference between experiment A2 and experiment A3 for 1986. Units are in °C. Contour interval is 0.25 °C.

Experiment	Resolution	Forcing fields	Vertical diffusion	Heat flux correction
C (Standard)	TDH (medium resolution)	Arpege wind stress Arpege heat flux Arpege water flux	$f(T,S)$	Yes
A1	TDH	Idem	$f(T,35‰)$	Yes
A2	TDH	Idem	$f(T,S)$	Not in WP
A3	TDH	Idem	$f(T,35‰)$	Not in WP
A4	TDH	Arpege wind stress Arpege heat flux LMD water flux	$f(T,S)$	Yes
A5	TDH	LMD wind stress LMD heat flux LMD water flux	$f(T,S)$	Yes
A6	TDH	Arpege wind stress Arpege heat flux (with diurnal cycle) Arpege water flux	$f(T,S)$	Yes
A7	TDH (increased vertical resolution)	Arpege wind stress Arpege heat flux Arpege water flux	$f(T,S)$	Yes
H1	TOTEM (high resolution)	Arpege wind stress Arpege heat flux Arpege water flux	$f(T,S)$	Yes
H2	TOTEM	ECMWF wind stress ECMWF heat flux Arpege water flux	$f(T,S)$	Yes
H3	TOTEM	ECHAM wind stress ECHAM heat flux Arpege water flux	$f(T,S)$	Yes

Table A.1. Summary of sensitivity experiments used in this study.

T tendency term $W.m^{-2}$	COARE box 1985-1994
Zonal advection	-1.1
Meridional advection	6
Vertical advection	0.1
Horizontal diffusion	-0.2
Forcing	-6.5
Entrainment	2.5
Net surface heat flux	13

Table A.2. SST tendency terms averaged over the whole COARE box during 1985-1994, for all gridpoints where the monthly average of the barrier layer thickness is greater than 20 meters (for the control experiment).

An OGCM Study for the TOGA Decade.
Part II: Barrier layer formation and variability

Jérôme Vialard and Pascale Delecluse
Laboratoire d'Océanographie DYnamique et de Climatologie (LODYC)
Case 100, Université Pierre et Marie Curie
4, Place Jussieu - 75252 Paris Cedex 05 - France

Revised version

Abstract

A set of OGCM experiments is used to investigate the processes responsible of barrier layer (BL) formation in the Pacific ocean. As in existing datasets, BL appears in our experiments both in the western Pacific (WP) and under the inter tropical convergence zone (ITCZ). In the WP, the BL displays a strong interannual variability linked to ENSO variability, in qualitative agreement with the observations of Ando and McPhaden (1997). In both the equatorial and 3°S-8°S bands, a subduction process is responsible for BL formation. In the equatorial region, it results from a strong downwelling near the salinity front created by convergence between central Pacific salty water and WP fresh water. In the southern region, the subduction of the South Equatorial Current (SEC) salty water involves mainly mixed layer retreat due to the freshening of the surface layer by rain and equatorial divergence of water from the eastward fresh equatorial jets. The formation of BL under the ITCZ is found to be mostly related to local precipitations.

The impact of the BL presence is then investigated. The BL interannual variability modifies the surface layer heat budget by switching on and off the entrainment cooling. The haline stratification traps most of the wind stress in the surface layer of the fresh and warm pool and induces strong eastward currents in response to Westerly Wind Bursts (WWBs). The overall effect of salinity stratification is to retain heat and momentum in the upper layer of the WP by restraining the exchanges with the cooler waters from below and from the central Pacific. The combined effect of zonal advection and mixing after a WWB results in an eastward shift of the thick BL regions along the equator. These properties of the BL structure might favor the growth of unstable air sea interactions in the central Pacific after a WWB.

B.1. Introduction

The western Pacific warm pool is characterized by some of the hottest surface water found in the world ocean (with annual temperatures around 29°C over large areas). This region is associated to an intense atmospheric convection, with precipitations ranging about 2 meters/year (Spencer, 1993). In the interval between convective events, calm winds and positive net heat fluxes associated to clear skies are observed. On the opposite, convective events are often associated with westerly wind bursts (hereafter WWBs), strong evaporative cooling and heavy rain (Anderson *et al.*, 1996). On a long term average, the western Pacific (hereafter WP) is characterized by weak easterly wind stresses (Hellermann, 1983), weakly positive heat fluxes (Oberhuber, 1988) and strong precipitations. These atmospheric conditions result in a very peculiar structure of the oceanic upper layer that was first described by Lukas and Lindstrom (1991). In a "barrier layer" (hereafter BL) situation, the mixed layer depth is controlled by the haline stratification. The cold water of the thermocline (usually just below the surface layer) lays around 30 meters deeper. The properties of the BL were studied in the part I of this paper, using OGCM experiments (Vialard and Delecluse, this issue). The salinity stratified layer between the surface layer and the top of the thermocline acts as a barrier against entrainment cooling and results in the trapping of wind momentum in the surface layer. The interplay of thin mixed layers and penetrative solar heat fluxes often result in the development of an inversion between the mixed layer and the BL (e.g. Anderson *et al.*, 1996). BL diminishes both entrainment cooling and solar heating of the surface layer, even allowing heat storage in the subsurface layer. This structure which diminishes the effects of atmospheric heat forcing on the oceanic upper layer might have a strong impact upon the air sea interactions.

The BL is not a sporadic oceanic structure but a climatological feature of the WP (Sprintall and Tomczack, 1992) displaying a strong interannual variability linked to ENSO variability (Ando and McPhaden, 1997, hereafter AM). This paper uses several OGCM experiments described in part I to explore the mechanisms responsible of the BL formation and large scale interannual variability. It is organized as follows. Section 2 gives an overview of the processes at work in the WP, where a BL is often present. Section 3 describes the salinity front separating the central and western equatorial Pacific in our experiments. Section 4 describes the mechanism driving the BL thickness (hereafter BLT) variability in the equatorial band. The impact of a WWB on the BL near the equator is also discussed in this section. Section 5 describes the mechanisms driving the BLT variability, south of the equator. Section 6 shortly discusses the BL formation processes in other regions. In the section 7, the effects of haline stratification in the low frequency variability of the WP are discussed. The main results of this study are discussed and summarized in section 8.

B.2. Background

A set of OGCM experiments of the tropical Pacific ocean was performed over the 1985-1994 decade to investigate the role of the haline structure in the physics of the warm pool (part I). The model is able to reproduce a BL in several regions. Two of them are located near the dateline - one near the equator and one in the 3°S - 8°S band - and correspond to regions of thicker BL (20 to 30 meters) in AM. The model also reproduces a thin BL under the inter tropical convergence zone (hereafter ITCZ), which is very sensitive to freshwater flux forcing. Thick BLT also appears around 120°W, 11°S but this result cannot be validated because of the lack of data in this area.

The modeled sea surface salinity (hereafter SSS) is in equilibrium between freshwater flux and entrainment in the WP (part I). The haline stratification inhibits entrainment cooling of the surface layer and acts against turbulent kinetic energy penetration into the ocean. This helps to set thin mixed layers, which result in a trapping of the atmospheric momentum and non solar heat fluxes in the surface layer. Only the solar heat flux penetration is not affected by thermohaline stratification: a significant part of solar heating is lost beneath the thin surface layer (Lewis *et al.*, 1990). This could explain how BL can persist over long periods in presence of a positive net heat flux in this region. This can also result in significant temperature inversions, associated to entrainment heating of the surface layer (Anderson *et al.*, 1996; Smyth *et al.*, 1996b).

These processes give an idea of how the BL structure can develop in the WP. The large scale easterlies help to set a deep main thermocline in the equatorial WP. Below the surface average 40 meters mixed layer, the temperature profile should be weakly stratified all the way down to

the heart of the thermocline (roughly defined by the 20°C isotherm, found around 150-200 meters). The fact that the temperature stratification starts around 30 meters below the mixed layer suggest that there is a heat source in the subsurface layer. This heat could be vertically redistributed over the subsurface layer by internal mixing for instance. Is the penetrative solar heat flux strong enough to supply the heat that creates this 20-30 meters BL? Or are subduction processes at work (Lukas and Lindstrom, 1991) to bring warm water in the subsurface layer of the WP? Our modeling results suggest that a salinity front created by the zonal convergence (Picaut et al., 1996) of western Pacific fresh water and central Pacific saltier water is essential in this subduction process. The existence and origin of this front is discussed in section 3. We find that a strong downwelling created near the salinity front by the zonal convergence is partly responsible of the deep thermocline near the eastern edge of the warm pool (section 4), and thus of BL formation in the equatorial band. In the 3°S-8°S band, the subduction of the South Equatorial Current (hereafter SEC) warm and salty water involves mainly mixed layer retreat due to the freshening of the surface layer by rain and equatorial divergence of water from the fresh equatorial eastward jets (section 5), like in Shinoda and Lukas (1995) results.

The experiments discussed in this paper are summarized in table 1. C is the control experiment, forced with the daily outputs of the Arpege AGCM T42 AMIP experiment (Déqué et al., 1994; Déqué, 1995). A4 uses the same forcing except for the freshwater flux forcing that originates from the LMD AGCM (Sadourny and Laval, 1984) AMIP experiment. Experiment A1 is similar to C, but the haline stratification is not accounted for in the vertical mixing computation. We present mostly the results of experiment C. Experiment A4 is used to investigate the sensitivity to the freshwater flux forcing. Experiment A1 is used to investigate the role of haline stratification. The results of two higher resolution experiments will also be mentionned. H1 uses the same forcing than C and has very similar results (part I). H2 uses different wind stresses and heat fluxes, and is useful to test the sensitivity to forcings other than the freshwater flux.

B.3. The salinity front

The average SSS structure that was presented in part I hides a strong time variability which can be seen in the figure 1. The strong SSS root mean square found under the ITCZ and southern Pacific convergence zone (hereafter SPCZ) can be linked to precipitations. The very strong (and certainly overestimated) SSS variability found near the equator and dateline suggests that there is a strong SSS gradient in this region. This is confirmed by an instantaneous snapshot of the modeled vertical haline structure along the equator during the last week of January 1990 (see figure 2) which can be compared with measurements at the same period and location in figure 5a of Kuroda and McPhaden (1993). During this period, the zonal convergence between the SEC and a surface eastward drift east of the dateline results in a strong salinity front in both data and model outputs. The horizontal structure of this front at the same date is presented on the figure 3. The front appears as the eastern boundary of the fresh water pool extending below the ITCZ and SPCZ in the WP. We define subjectively the "fresh pool" as the volume of fresh water lying west of this front between 5°N and 5°S (see figure 3 for an example). The frontal zone is almost a permanent feature in the model results (as it can be spotted in time longitude sections displayed in the figure 4a). The salinity front cannot be attributed to a bias arising from the forcing of the control experiment. It indeed appears in the experiments A4 and H2 using respectively different freshwater flux and wind stress forcings.

This salinity front has been observed at 165 East with TAO mooring (Sprintall and McPhaden, 1994) and by an equatorial cruise (the Flupac campaign: Eldin et al., 1996). The surface salinity gradient in both Eldin et al. (1996) and Kuroda and McPhaden (1993) is of the same order than the simulated SSS gradient (respectively 0.17 and 0.13 psu per degree of longitude whereas the maximum simulated SSS gradient in the frontal zone is around 0.2). Despite the few direct observations of this salinity front, a recent work by Picaut et al. (1996) suggests that it exists in the ocean. The studies of Picaut et al. (1996) and Delcroix and Picaut (1997) suggest that this SSS frontal zone materializes the zonal convergence between central and western Pacific surface water masses. There is indeed a permanent westward transport of water masses within the SEC in the central Pacific, where evaporation dominates over precipitations. On the opposite, the seasonal Australian monsoon, the occasional WWBs and

the interannual variability of the easterlies cause an intermittent eastward surface flow in the WP (e.g. Reverdin *et al.*, 1994; McPhaden *et al.*, 1992), where the atmospheric convection leads to strong precipitations. The result is a zonal convergence of the western Pacific fresh water and central Pacific saltier water around the dateline. The exact longitudinal position of this convergence zone is subjected to a large interannual variability. This variability and the analysis of its driving mechanism are presented in the following section.

B.4. Thermohaline structure variability in the equatorial band

B.4.1. Sea surface salinity variability

a) The sea surface salinity in the equatorial band

In contrast with SST (which is damped toward observed values), SSS is left free in our model, and is thus a good indicator of its variability. The examination of the root mean square of the simulated SSS in experiment C (figure 1) shows that the highest variability is found in the equatorial band. Figure 4 shows a time - longitude evolution of the simulated SSS in this band (2 °N - 2 °S). We also used SSS measured by opportunity merchant ships (Hénin and Grelet, 1996) along four navigation tracks to compute a similar diagram from observations. This last figure has to be considered with care due to the large spatial gaps between the tracks and the extensive interpolation thus used (especially in the 92-94 period where the data are sparse).

Both model and data agree in an eastward displacement of the western Pacific "fresh water pool" during El Niño events, whereas the salty water from the central Pacific moves westward during La Niña. The fresh pool migrates west of 165°E during 1985, in agreement with La Niña situation. It migrates as far east as 145°W during the 1986 - 87 El Niño in model results, whereas it does not seem to cross 160°W in observations. Both model and data exhibit a westward migration of the fresh pool at the onset of the 1988 - 89 La Niña. From 1988 to 1992, a progressive eastward migration of the fresh pool is visible in both model and data, coherent with the transition from La Niña to El Niño state via the "normal" 1990 year. After 1989, the model stays in an anomalous fresh state, with low salinity crossing the dateline. Comparison of the simulated and observed SSS along several ship tracks crossing the equator indicates that the zonal displacement of the "fresh pool" region is mostly trapped in the 5°N - 5°S band. The main bias of the experiment is a too strong westward displacement of the fresh water pool during El Niño events. This is confirmed by the comparison of the simulated SSS with the measured one along the main Pacific Ocean ship tracks and can clearly be attributed to the Arpege weak easterlies (part I).

The one degree zonal resolution of the model lets see a strong salinity front between western Pacific fresh water and central Pacific salty waters. The coarse resolution of the available salinity data does not allow to see the highly mobile salinity front. The existence of this frontal zone might be related to the large scale convergence between the salty westward SEC and the fresh eastward drifts associated to the reverses of the easterlies in the WP (Picaut *et al.*, 1996; Delcroix and Picaut, 1997). This hypothesis of a zonal convergence zone has been tested by computing trajectories driven by zonal equatorial currents, following Picaut *et al.* (1996)'s method. Lagrangian drifters trajectories were computed using modeled currents at 5 meters, averaged between 4°N-4°S. Their trajectories are supposed to give a representation of water masses flow in the equatorial band (see figure 5a). Except during La Niña periods, all the trajectories end by adjusting their position to the salinity front. This means that the currents have a tendency to transport water parcels westward in the central Pacific (where evaporation is strong) and eastward in the WP (where precipitations are strong), leading to the buildup of a salinity front. The equatorial front position also corresponds very well to the 28.5°C isotherm position in the experiment. The fact that there is a salinity front in the convergence zone and no obvious temperature front is intriguing. East of the front, temperature is the result of balance between westward water transport, entrainment of subsurface colder water and local forcing. Water masses heat up slowly as they travel west until they meet western Pacific water. The surface temperature of the warm pool is mostly determined by a local balance. The mechanism allowing these independent water masses to meet in the convergence zone at the same temperature (around 28.5 °C in the model) has to be explored.

b) Mechanism driving SSS variability in the equatorial band

The previous qualitative approach, proposing zonal advection as a mechanism for the salinity front and its movements, can be confirmed by a quantitative analysis of the model salinity equation. A mixed layer budget method has been developed to compute the different terms acting on the temperature and salinity in the model mixed layer (see appendix A in part I). Table 2 displays the average tendency terms driving the mixed layer salinity for the 85-94 period. These tendency terms are integrated over three 10° wide boxes moving along with the frontal region. Tendency terms in the frontal region (defined as the 34.6 isohaline position ± 5°) are given separately for eastward and westward propagation of the eastern edge of the fresh pool. They feature zonal, meridional and vertical advection, horizontal diffusion, forcing and entrainment.

In the frontal region, the zonal advection term explains most of the SSS variability. It is indeed the only term working in opposite directions between eastward (decreasing salinity) and westward (increasing salinity) propagation of the front. The large scale zonal current is thus the most determinant factor in driving the front position. The other terms of the SSS equation are not negligible near the front. Their contribution to salinity variability is however small. The overall effect of meridional advection in the equatorial band is to decrease salinity. This effect increases during eastward propagation (-0.231 psu/month instead of -0.132 psu/month). However, the increase of the entrainment term (0.298 psu/month instead of 0.195) due to the strong vertical shear associated to eastward jets cancels this effect. The salinity forcing term is not significantly modified between eastward and westward propagation. The salinity structure and freshwater flux are not realistic enough to study precisely the importance of the other terms: only the importance of zonal advection can be considered robust in respect of what happens in the ocean.

West of the salinity front, the fresh surface water is mostly under the influence of entrainment and forcing. These two terms are nearly in equilibrium most of the time. The strengthening of one of them, under the influence of heavy rain or wind bursts, will cause the rise of low or high salinity patches in this region. East of the front, the salinity variability is very weak.

B.4.2. Barrier layer variability and formation mechanism

The figure 6a is an illustration of the time longitude evolution of BLT in the equatorial band. The BL displays large interannual migrations. It is localized west of 165 East during the 1985 and 1988 - 1989 La Niñas. In El Niño phases, it moves eastward. In its most extreme position, the BL forms between the dateline and 140W in 1986, 1987 and 1992 (mature El Niños). It also disappears from the equatorial region at several occasions (April 1988, June - July 1992, June - August 1993). This sequence is in agreement with the time longitude diagram of BL computed from CTD profiles by AM (figure 6b). The strong variability of simulated BLT is evidently linked to the SSS front position (see figures 4a and 6a) (note that Tomczack (1995) has observed the development of a BL after the passage of a salinity front, but at a much thinner scale). BL always appears in the fresh pool region, west of the salinity front. Meanwhile, BL is not present in the far western Pacific during the El Niño phases. There is a very good coincidence between BL regions (and more generally the salinity stratified regions) and zonal current shear between the surface and subsurface layer (see figure 5b). It can be explained by the fact that salinity stratification in the upper meters of the WP inhibits the wind momentum penetration in deeper ocean (part I; Chen and Rohstein, 1991). By capturing most of the wind forcing, the surface layer develops a very energetic response. Zonal shear in the 70 upper meters of the fresh pool is almost always positive (i.e. the surface moves east relatively to the underlying layer under the effect of westerly anomalies of the wind stress). The salinity stratification insulates the fresh upper layer from the underlying and surrounding salty water. The western Pacific surface water can be seen as a huge fresh water lens floating on the central Pacific salty water, and sliding on it when pushed by a WWB, the penetration of Australian monsoon or interannual anomalies of the wind stress. The BL acts as a barrier in two ways. It brakes upward mixing of cold thermocline water as well as it cramps downward mixing of wind momentum. An alternate view of this sheared current structure can be provided by the difference between the trajectories driven by the surface equatorial speed and the subsurface (figure 5a). While trajectories driven by the surface zonal current all end up by converging into the SSS frontal zone, the subsurface flow (at a 70 meters depth) brings them further west. This can be explained by the fact that the haline stratification in the WP shelters the subsurface

waters of the SEC from the westerly anomalies of the wind stress. This layered structure of the flow in the WP (eastward flow in the 40 first meters, westward flow deeper, until the depth of the eastward flowing EUC) has been described by many authors (e.g. Kuroda and McPhaden, 1993; McPhaden et al., 1992). Boulanger et al. (1997) computed a long wave equatorial decomposition of the simulated variability for the TOGA decade, using the higher resolution H1 experiment and exactly the same forcing than our study (see table 1). Results of the C and H1 experiments are close enough to extend their results to our lower horizontal resolution study. It is interesting to note that there is a good visual correlation between the Kelvin wave coefficient of Boulanger et al. (1997) and the thickness of the BL. The BL is thick when and where the oceanic structure is typical of the downwelling Kelvin wave structure. On the opposite, it is thin or missing when the oceanic structure is typical of upwelling Kelvin waves.

We will now explore which specific processes lead to the BL formation near the salinity front. Figure 7 represents a longitude - depth plot of the average hydrographical conditions around the frontal region. Figures 7a and 7b are averaged over the months in which a BL thicker than 10 meters appears west of the front (110 occurrences), whereas figures 7c and 7d are representative of the months where no BL forms west of the front. Note that the speed of the averaging frame is negligible (~3 cm.s^{-1}) and that the mean structure was verified to accurately depict the instantaneaous vertical structure near the front. Months when a BL appears are associated with a strong zonal convergence of eastward jets and the SEC in the upper layer of the frontal region. This convergence is compensated by a strong downwelling of 28°C water (with average values up to 1.2 m.day^{-1}) just east of the salinity front. This downwelling is associated to a deepening of the top of the thermocline in the frontal region (around 75 meters). This situation is severely disturbed in figure 7, which is characterized by upwelling Kelvin waves near the frontal region in Boulanger et al. (1997) analysis. These Kelvin waves are associated with westward current anomalies at the surface: the flow is westward across the front over the 25 first meters. The strong zonal convergence in the surface layer disappears. Due to increased upwelling, the top of the thermocline crops up toward the surface (50 meters), coming close to the halocline depth.

The two previous pictures are respectively remarkably similar to the conditions measured along the equator during the January - February 1990 R/V Natsushima cruise (Kuroda and McPhaden, 1993) and the February 1989 cruise. This agreement comforts us in proposing the BL scenario summarized in figure 8 schematic view. Convection occurs above the warm pool region and strong showers freshen the surface in the WP. This convection is associated with convergence of steady easterlies and intermittent WWBs. The westerly winds in the WP drive eastward jets in the upper ocean. These jets overshoot eastward of the atmospheric convergence zone. This might be due to the eastward transport of momentum by the Kelvin waves, or to the equatorward convergence of zonal momentum associated to eastward jets. The haline stratification inhibits the downward penetration of eastward momentum, resulting in a strong positive vertical shear. The convergence of western Pacific fresh water and central Pacific salty water gives rise to a salinity front. The convergence of zonal currents in the front region is balanced by a strong downwelling just east of the front. Such a downwelling acts to deepen the upper thermocline under the front (as it can clearly be seen in the January - February cruise of the R/V Natsushima (Kuroda and McPhaden, 1993)). The westward movement of subsurface water relative to the surface layer (see figure 5) supplies the BL with warm salty water downwelled near the front. This picture of fresh surface jet moving eastwards over a depressed upper thermocline interacts with the locally or remote forced Kelvin waves. Downwelling Kelvin waves reinforce this mechanism (1986-1987 and 1989 - mid 1992). Upwelling waves act against it (early 1988, mid 1992 and mid 1993) (Boulanger et al., 1997) by rising up the thermocline and suppressing the eastward jet (upwelling Kelvin waves are associated to westward zonal speed anomalies).

We can summarize our scheme as follows. The surface fresh water of the WP traps most of the WWBs momentum and slides eastwards over the westward moving underlying water. When this fresh tongue superimposes a deep thermocline, it results in a thick BL. The thermocline deepening results from the zonal convergence in the front, reinforced by downwelling Kelvin waves. It is important to note that this mechanism is both related to the fresh equatorial jet mechanism (Roemmich et al., 1994) and to the subduction mechanism (Lukas and Lindstrom, 1991; Shinoda and Lukas 1995). However, it involves both downwelling and

vertical shear whereas the one proposed by Shinoda and Lukas (1995) for the 10°S - 0°S band only involves mixed layer retreat. We have not investigated the potential role of the pressure gradient associated to the salinity front in driving the eastward jet (as proposed by Roemmich *et al.*, 1994).

Several mechanisms allow the subsurface water in the BL region to stay at the same temperature than the surface water. When reaching the frontal region, the central Pacific water is already around 28.5 °C (which is not far from the hottest temperature developing in the Warm Pool). It is then subducted under the western Pacific fresh pool. Meridional convergence of northern and southern warm pool water between 40 and 80 meters might provide a second warm water source in the subsurface layer west of the front. The penetrative solar heat flux represents a third heat source for the subsurface waters of the fresh pool, whereas the budget of the surface layer is near zero or negative from both local or climatological estimates (part I). The surface layer might stay at the same temperature than the underlying layer because entrainment brings heat upward.

West of the front, the BLT variability is controlled by the competition between the sloping up of the upper thermocline and the changes in the mixed layer depth associated with rain showers (Chen and Rohstein, 1991; You, 1995, Tomczack 1995) or wind bursts. We think that BL disapears west of 160° East during El Niños for three reasons. During El Niños, the convection zone of the WP moves eastward. This is associated to a change in the large scale wind stress pattern which drive a sloping up of the heart of the thermocline in the far western Pacific. Furthermore, the downwelling associated to the zonal convergence does not supply the subsurface of the far western Pacific with warm water any more, having now migrated far away to the east. These two facts result in a rise of the top of the thermocline in the WP. The convective zone having migrated east, the wind stresses are stronger than usual in the far western Pacific. This stronger wind stiring drives deeper mixed layers. The combined effect of shallower thermocline and deeper mixed layer results in the vanishing of the BL from the far western Pacific.

Some uncertainties and shadow areas remain in our study. First, the strong correspondence between the salinity front and the eastern edge of the thick equatorial BL region does not appear in AM. This might be due to the poor resolution

(10° in longitude x 3 months) and strong filtering (1/4,1/2,1/4 in both time and longitude) applied to their dataset. It might also correspond to a BL formation mechanism which does not appear in our control experiment but is suggested by a sensitivity test (experiment A4, with the freshwater flux from the LMD AGCM). The salinity frontal zone still exists in the A4 experiment. It is however weaker than in C experiment, because casual low SSS patches appear east of the front. The LMD AGCM indeed produces strong precipitations east of the Arpege wind stress driven salinity front. The result is that BL can occasionally form east of the front. This is a clue to a BL formation mechanism which was not present in our standard experiment. Occasional rain showers over the thick isothermal layer of the central Pacific could create freshwater lenses associated with a thick short-lived BL. Another question is arisen by the exact role of Kelvin waves. The analysis of Boulanger *et al.* (1997) taught us that oceanic structures that projected well on downwelling (upwelling) Kelvin waves were propitious (unfavorable) to BL formation. The WP is however the region where the Kelvin waves are forced (by WWBs). It is thus difficult to say what is the exact role of Kelvin waves in the BL formation in this region where remote and local forcing are difficult to distinguish.

B.4.3. Sensitivity of barrier layer to synoptic atmospheric forcing

The WWBs are believed to play a key role in triggering the ENSO events. They produce strong vertical shear and intense mixing that can potentially destroy the BL structure (Lukas and Lindstrom, 1991), and modify the local surface layer heat budget. They are also important in generating downwelling Kelvin waves which modify the zonal current and vertical stratification structures as they propagate eastward. We performed sensitivity experiments to explore the local and remote effects of an intense WWB on the BL and SSS front structures. To clearly discern the effect of the wind burst from the background circulation, we performed an "Arpege seasonal cycle experiment": W0. The 1985-1994 daily Arpege forcing was averaged to produce a 365 day mean forcing, and the surface temperature was damped toward a monthly average of the 1985-1994 Reynolds (1988) SST. Idealized anomalies of the zonal wind stress (Harrisson and Giese, 1991) were then added to this mean forcing. They were centered on the

equator, extending over a 20° longitude, with a 0.05 N.m⁻² amplitude lasting for 20 days.

The W0 experiment displays a seasonally varying BL in the equatorial band. This seasonal cycle is weaker than the interannual variability. We will not focus on the BL cycle of experiment W0, but only use it as a control. The W0 experiment produces a tight salinity front and thick (around 30 m) BL in the vicinity of 170°E, during August and September. The 20 day wind bursts were centered the 20th of august, at 140°E, 160°E and 180°E. The overall effect of a WWB on the BL structure is depicted by the figure 9 (the WWB centered at 160°E beeing taken as an example). Locally, the WWB produces a strong vertical shear and an energetic turbulent mixing input in the surface layer which result in a deepening of the mixed layer. This turbulent kinetic energy production is often sufficient to mix the upper layer down to the thermocline, thus destroying the BL in the region of the forcing (see figure 9b). An equatorial wave associated to positive zonal speed anomalies is radiated eastward (toward the frontal zone). We did not investigate further the exact nature of this wave which propagates at the first Kelvin mode wave speed. This wave induces a slight (500 to 1000 km) eastward advection of the salinity front, and of the associated thick BLs. The overall result of a WWB in the fresh pool is an eastward shift of the thick BL region. This effect might appear quite weak (only a few degrees of longitude displacement of the BL region) compared to the interannual variability of the BL. We must however keep in mind that we are in a forced framework, and that any atmospheric feedback that might favor the BL growth further east after a WWB is not accounted for.

At the light of these results, we suggest that the combined effect of a wind burst and of the haline vertical structure might result in the short-term SST anomaly growth in the vicinity of the dateline spotted in Rasmunsson and Carpenter (1982) ENSO composite. A WWB first occurs in the WP (around 150°E or 160°E). Its local effect is to destroy the BL and to switch on the entrainment cooling. This induces a slight cooling of the SST in the WP. Meanwhile, the eastward propagating current anomaly results in both a slight positive SST anomaly near the dateline because of eastward zonal advection of warm pool water (Picaut and Delcroix, 1995) and the development of a BL in the same region. This positive SST anomaly persists because the newly formed BL cuts off the entrainment cooling. If this warming near the dateline is sustained long

enough, its combined effect with the cooling in the WP might result in an eastward displacement of the atmospheric convective activity. Eastward current anomalies are then increased by the trapping of westerly wind momentum in the surface layer by the haline stratification. The haline stratification thus potentially acts to sustain the growth of SST anomalies in the central Pacific. This hypothetical scenario has however to be confirmed by observations and coupled models.

B.5. Thermohaline structure variability southern of the equator

B.5.1. Sea surface salinity variability

The other region in which BL appears in the WP is situated in the 3°S - 8°S latitudinal band. Figure 10 displays a time longitude evolution of the SSS in this band. The figure 11 displays the zonal and meridional mixed layer salinity advection terms. In contrast with the equatorial region where zonal advection is responsible of both eastward and westward movement of the salinity front, the situation is asymmetric south of the equator. Zonal advection is still responsible for increasing salinity (westward front movement) (see figure 11a). Decreasing salinity corresponding to an eastward movement of the front is explained by the meridional advection (figure 11b).

This behavior can be interpreted as follows : the westward movement of the freshwater in the 3°S - 6°S band is due to the zonal advection by the SEC. The asymmetry in the zonal advection term is caused by the difference in meridional scale between the SEC and the equatorial jets (figure 12). Most of the eastward jets are trapped in the equatorial region between 3°N - 3°S (Delcroix et al., 1992). On the contrary, the SEC has a broader latitudinal extension, between 4°N and 6°S. The 3°S - 6°S band is thus always under the influence of the SEC and does not see the equatorial jets (a SECC exists in the model but rarely extends as far east as the front in the 3°S - 6°S band). It can however indirectly be affected by these "fresh equatorial jets". Eastward propagation of the fresh equatorial tongue is followed by a return of the SEC. Equatorial divergence then becomes active, and evacuates some of the equatorial freshwater towards North and South. Decrease of salinity in the 3°S - 6°S band is mostly caused by the divergence of equatorial freshwater. The lesser influence of zonal advection in the 3°S - 6°S band results in a

looser salinity front between the central and western Pacific. Once again, whereas advection processes are dominant in the frontal zone, forcing and entrainment are the main processes further west, in the fresh pool.

B.5.2. Barrier layer variability and formation mechanism

The notion of Lagrangian "water columns" drifting in a vertically homogeneous surface layer current is not valid near the equator because of the vertical shear. In contrast with the equatorial situation, both the vertical shear and the meridional flow are weak in the 3°S - 6°S band. The water columns in this band are vertically homogeneously advected from the central Pacific toward the WP, as simulated by Shinoda and Lukas (1995). The one dimensional mixed layer processes are thus the dominant mechanisms driving the surface layer structure along the water columns trajectories. As it can be seen in figure 10a, the water columns begin to warm up (by solar heating) far east off the SSS front. When reaching the western region, they receive freshwater in the upper layer as explained above (meridional advection and freshwater flux). This freshening of the surface layer over a thick isothermal layer is associated to mixed layer retreat and BL formation (figure 10b). The BL formation is thus conditioned both by freshwater supply and one dimensional mixed layer processes. As suggested in Shinoda and Lukas (1995), the BLT also seems to be sensitive to equatorial Rossby waves (their thermocline depth signal is strong near 4° N and S). Strong upwelling Rossby waves cross the eastern edge of the fresh pool at the end of 1986, mid 1987 and mid 1993 (Boulanger et al., 1997). All these periods are associated with a shrinking or a vanishing of the BL near the front.

This mechanism is very similar to the one described by Shinoda and Lukas (1995). It is important to note that equatorial divergence of surface fresh water complement their mechanism. This mechanism, where subduction is associated to a mixed layer retreat along lagrangian trajectories of water column, has to be differentiated with subduction in the equatorial zone (the latter being associated to three dimensional dynamics involving vertical shear and downwelling near the SSS front).

B.6. Other barrier layer formation regions

The simulated BLT was shown to be quite sensitive to the prescription of the water flux in part 1 (experiment A4). The stronger precipitations in A4 result in thicker BL. Except under the ITCZ (where A4 displays a 10 meter BLT whereas C has none), thick BL regions are similar in the two experiments. Two regions are found in the WP (both in our experiments and in AM climatology), whose formation mechanisms have been discussed in parts 4 and 5. Another region is found around 120°W, 12°S in both C and A4 experiments but does not appear in AM. Let us now discuss the simulated BL formation process under the ITCZ (experiment A4) and around 120°W, 12°S.

The fact that BL appears under the ITCZ only when stronger precipitations are used suggests that direct freshwater forcing is crucial to BL formation in this region. This is confirmed by the analysis of BL time series (figure not shown): BL is observed to develop during periods of strong precipitations (and to last some weeks after). Yet, correlation around 0.8 between the monthly mixed layer depth and the surface buoyancy forcing indicates a strong control of the mixed layer depth by the precipitations (which dominates buoyancy forcing in this region). The strong rain events are associated to a mixed layer retreat above a still deep thermocline. We suggest that the mechanism allowing the surface layer to keep the same temperature than the underlying layer is partly the same than in the warm pool: the thin mixed layer loses a significant part of penetrative solar heat flux at the bottom. The negative heat flux associated with the rain drops (which is not accounted for in the model) might even favor the cooling of the surface layer. In contrast with the equatorial region, there is here no subsurface heat source associated to the subduction of warm water. That might explain why the BL is shorter lived under the ITCZ (~ 2 monthes) than in the WP (~ 1 year).

Let us now investigate the BL formation process around 120°W, 12°S. We recall that the existence of BL in this region cannot be validated because of the lack of data in the composite of AM there. The existence of BL in this region cannot be considered as the result of the biases of Arpege precipitations as the same feature appears in experiment A4, which uses another freshwater flux. The modeled BLT variability in this region is essentially a seasonal phenomenon (whereas the interannual timescale was dominant in the WP). An analysis using Lagrangian trajectories of surface water columns (figures not shown) suggests that the following

mechanism is at work in this area in our experiments. During the northern winter, the southward displacement of the ITCZ is associated with a freshening of the surface water in the eastern equatorial basin (both in our model results and in Levitus, 1982). When the ITCZ moves north again, the southern part of this fresh water pool is advected southwestward by the combined action of the SEC and the equatorial divergence. The overall effect of the surface forcing on the water columns is a cooling along their trajectory. The upper water column thus cools down as it moves toward regions where the thermocline is deeper. The haline stratification however acts against the downward penetration of convective overturning. This results in an halocline deepening at a slower rate than the underlying thermocline, while the fresh water columns travel south. Thick BL develops around 120°W, 12°S during the northern summer as the result of this process.

B.7. Salinity effect in the variability of the western Pacific

B.7.1. Impact on the surface layer heat budget

To investigate the effect of BL interannual variability on the surface layer heat budget, we divided the oceanic state into three categories. East of the front, the situation is typical of the "central Pacific" (high salinity, equatorial upwelling, deep mixed layer, east west temperature gradient, etc...). West of the salinity front, either a BL is present ("western Pacific" situation) or there is no BL ("far western Pacific" situation). Our definition of these three categories is not geographic, but moves in phase with the interannual variability. The mixed layer budget method (described in the appendix A of part I) is used to compute the tendency terms driving the SST variability in several boxes which feature two 2°N - 2°S boxes extending between 140°E and 160°E (Box I), 170°W and the dateline (Box II). Depending on the interannual variability, these boxes are found in a "central", "western" or "far western" Pacific situation. Table 3 summarizes the characteristic values of each tendency term for the different situations in Boxes I and II.
• The "Central" Pacific situation can be found in Box II. From mid 1988 to mid 1989, La Niña situation is dominant over the Pacific ocean. The salinity front is situated west of 170°E, and Box

II thus experiences "central" Pacific conditions. It is characterized by a deep mixed layer in which temperature is the result of an equilibrium between strong entrainment (-47 W.m^{-2}), zonal advection (-24.5 W.m^{-2}) and forcing (61.5 W.m^{-2}).
• The "Far western Pacific" situation (no BL) is found in Box I during the 1987 warm episode. The thick BL region has migrated eastwards. The tendency terms are much weaker in this situation than in the "central" Pacific situation (around 0.15 °C.month^{-1} instead of 0.55 °C.month^{-1}), due to reduced temperature gradients. The dominant terms in the mixed layer temperature budget are the entrainment (cooling of -10 W.m^{-2}) and the meridional advection (warming of 7 W.m^{-2}). We will not discuss the role of meridional advection as it is not systematically dominant in "far western" Pacific situation. However, in this situation, as in the "central" Pacific, entrainment cooling of the surface layer is present.
• The "western" Pacific situation is found both in Boxes I and II. In 1989, the BL region has migrated westwards with the warm pool, due to La Niña situation. BL is then present in Box I with an average thickness of 17 meters over the period. There is no entrainment cooling, unlike during 1987 when no BL was present. Entrainment flux is even slightly positive. It is important to note that the tendency term due to external forcing is near zero whereas the net surface heat flux is around 16 W.m^{-2} over the period (the flux correction term being nearly zero). This underlines once again the effect of penetrative solar heat flux. In 1991, a BL associated to the eastward migration of the fresh pool is present in Box II which is in "western" conditions. Tendency terms (including entrainment) are now much weaker than in the "central" Pacific situation. The external forcing tendency term always tends to compensate the other dominant terms (mostly zonal and / or meridional advection) via the heat flux correction term. The importance of this correction term compared to the other terms does not permit to clearly identify the dominant processes in the western Pacific mixed layer temperature equilibrium. The contrast between entrainment cooling in "central" and "western" Pacific is however significant enough to conclude that the equilibrium is radically different in each case. The fact that entrainment can be switched on and off by the BL presence could be important in ENSO scenarios (Lukas,

1988). During El Niño periods, the eastward migration of the BL zone is associated with the uprising of entrainment cooling in the western part of the basin. This effect might contribute to the decrease of SST there. The convection cell would thus move eastwards toward the highest SST zone. This hypothesis is difficult to test in a "forced" framework and will be investigated with a coupled model in near future.

- When extending the above analyses to the whole COARE region, the impact of BL interannual variability on entrainment is less significant than in the equatorial band. The BL does not seem to be a determinant factor in the mixed layer temperature budget of the whole COARE Box. Nevertheless a fully coupled system is required to get a better insight of the determinant processes in the COARE surface temperature equilibrium.

B.7.2. Impact of haline stratification on fresh pool displacements

Picaut *et al.* (1996) have demonstrated that the zonal displacement of the eastern edge of the WP is mostly driven by zonal advection. It is shown in part I that the haline stratification enhances the zonal current response to wind forcing in the WP by trapping the wind stress in the surface layer. We have tested the sensitivity of the warm and fresh pool zonal displacements to the effects of haline stratification. An experiment was conducted where the vertical mixing is computed with the thermal stratification only (experiment A1 in table 1). The figure 13 shows a time - longitude plot of the SSS and surface zonal currents in control and A1 experiments. The momentum of eastward wind anomalies is dispatched over a thicker layer in A1. This results in slower fresh equatorial jets. The eastward movements of the fresh pool during El Niños are thus smaller in this experiment. This can be spotted in the location of the salinity front (which for example does not cross 160°W whereas it reaches 140°W at the end of 1986 in the control). The damping toward the observed SST does not allow to see clearly the haline stratification effect in the displacement of the warm pool. This sensitivity experiment however suggests the following schematic view. Haline stratification acts as a ball bearing under the upper layer of the western Pacific warm pool: it emphasize its zonal movements driven by eastward wind anomalies.

B.8. Summary and Discussion

Summary

The results described in part I show that the BL structure is important in setting the heat budget of the surface layer. BL was notably shown to cut down the entrainment cooling of the surface layer in the vicinity of the equator. In part II the driving mechanism of BL formation and variability in the Pacific ocean are investigated. BL appears mostly in two regions. Both are located in the WP, one in the equatorial band and the other in the 3°S-8°S band. The formation mechanism in the equatorial band is found to be mostly linked with a sharp salinity gradient between the 35.2 psu waters of the central Pacific and the "fresh pool" region of the equatorial WP. This frontal zone has been observed in equatorial measurements of salinity (Kuroda and McPhaden, 1993; Sprintall and McPhaden, 1994). It is linked to the convergence between the westward advected central Pacific salty waters and occasionally eastward advected western Pacific fresh water, which results from a basin scale wind forced equilibrium and moves longitudinally in phase with interannual variability (Picaut *et al.*, 1996). This frontal zone separates two regions of the equatorial band characterized by fully different vertical stratification. East of the front, the stratification is typical of the central Pacific with a deep mixed layer limited by thermal stratification. West of the front, the model reproduces a BL situation: a shallow halocline (and mixed layer) over a deep thermocline (Lukas and Lindstrom, 1987). This is the result of the combined effect of eastward shear west of the front and downwelling near the front, which supplies the subsurface layer of the fresh pool with 28°C surface water (figure 8). This subsurface heat source as well as the penetrative solar heat flux contribute to maintain a thermocline deeper than the mixed layer (barrier layer) in the equatorial WP. South of the equator, we found the BL formation process described by Shinoda and Lukas (1995). Water columns are advected westward in the SEC southern branch. They are already very warm when they reach the WP where they get freshwater in the surface layer from both precipitations and meridional advection. A thick BL forms associated to a salinity controlled mixed layer retreat. BL also appears under the ITCZ. We find it to be strongly controlled by precipitations and maintained by penetrative solar heating. Finally, thick BL also appears in our experiments around 120°W, 12°S where there is no data to validate its existence in the

ocean. BL could develop there as the result of southwestward advection of freshwater patches created near the Ecuadorian coasts by the seasonal migration of the ITCZ.

The interannual variability of the BL is shown to modify significantly the surface layer heat budget of the WP, mostly by cutting off the entrainment cooling. The haline stratification is shown to take an active part in the fresh pool displacements by trapping the wind momentum in the surface layer, thus resulting in more energetic eastward jets.

We also suggest that the BL layer structure could favor the growth of an ocean atmosphere coupled instability. In our idealized experiments, the overall effect of a wind burst in the fresh pool is a slight eastward shift of the thick BL zone. The effect of a wind burst is to destroy locally the BL and to favor the development of negative SST anomalies. East of the WWB, remote forcing favors the eastward advection of the eastern edge of the warm / fresh pool. A positive anomaly of SST and BLT might thus develop near the dateline. The BL insulating effect might last long enough to maintain this SST anomaly one or two months, thus allowing an eastward migration of the atmospheric convective activity. The haline stratification should then favor the surface layer zonal current response to the growth of eastward wind stress anomalies...

Discussion

The modeling framework of our study is a source of uncertainties. The frontal zone between the central and western Pacific waters is sometimes very pinched. Direct observations of this front are too sparse to conclude that such a tight structure always delineates the eastern edge of the warm pool. Two studies by Picaut et al. (1996) and Delcroix and Picaut (1996) using several surface current datasets suggest that equatorial zonal convergence of SEC and warm pool waters result in such a structure in the ocean. The resolution of our model might however not be sufficient to study the baroclinic compensation of this intense surface convergence. Other numerical aspects of our large - scale experiments might also not be adapted to study the fine scale processes near the front (horizontal diffusion coefficient, spatial filtering of turbulent kinetic energy equation tendency terms, etc...). Another major uncertainty concerns the current and the thermohaline simulated fields. The simulated BL around 120°W, 12°S might for instance be a model bias (we have no data to validate it). The robustness of the described processes to several changes in the forcing fields (part I) however suggests that the model results account at least for a part of what happens in the real world.

Some shadow areas however remain. First, it is difficult to find out which of the local and remote forcing is more important in driving thick BL near the equatorial SSS front. Although we find several large scale BL formation processes, there are also smaller scale (Tomczack, 1996) and higher frequency (Anderson et al., 1996) BL formation processes. It is difficult to say whether these small scale processes can contribute to the large scale and low frequency variability of the BL. Only COARE studies and meso scale modeling will teach us more about that.

Finally, we found the BL to be a very peculiar oceanic structure. It inhibits both SST cooling (by cutting out entrainment cooling) and solar heating (an important part of the penetrative solar flux can be lost beneath the thin mixed layer). Furthermore, it amplifies the dynamical response of the surface layer by trapping the wind momentum in the surface layer. This structure allowing slow SST growth (by favoring storage of heat in the subsurface and positive entrainment) and delaying the cooling after a wind burst might interact strongly with the atmospheric physics. We will thus continue this study and check whether the aforementioned processes significantly affect air sea exchanges in a the coupled framework. We will then try to investigate whether the BL structure can favor the growth of an ocean - atmosphere coupled instability, as suggested in the "Summary" part.

B.References

Anderson, S.P., R. A. Weller and R.B. Lukas, 1996, Surface buoyancy forcing and the mixed layer of the western Pacific warm pool: observations and 1-D model results, *J. Clim.*, in press.

Ando, K. and McPhaden, M.J., 1997, Variability of surface layer hydrography in the tropical Pacific ocean, for submission in *J. Geophys. Res.*

Boulanger, J.P., P. Delecluse, C. Maes and C. Levy, 1997, A high resolution OGCM simulation of the tropical Pacific ocean during the 1985-1994 period. Part I: long equatorial waves. *Mon. Wea. Rev.*, in press.

Chen, D. and L. M. Rohstein, 1991, Modeling the surface mixed layer structure in the western equatorial Pacific, unpublished manuscript (*TOGA notes*, 2, 13-16).

Delcroix, T., G. Eldin, M.-H. Radenac, J. Toole and E. Firing, 1992, Variation of the western equatorial Pacific Ocean, 1986-1988. *J. Geophys. Res.*, 96 (suppl.), 3249-3262.

Delcroix, T., J. Picaut, 1997, Zonal displacement of the western equatorial pacific fresh pool, submitted to *J. Geophys. Res.*

Déqué, M., C. Dreveton, A. Braun and D. Cariolle, 1994, The ARPEGE/IFS atmosphere model : a contribution to the french community climate modelling, *Climate Dyn.*, 10, 249-266.

Déqué, M., 1995, Sensitivity of the Météo-France/CNRM GCM to horizontal resolution, Proceedings of the first international AMIP scientific conference, *WMO/TD-No. 732*.

Eldin G., M.H. Radenac and M. Rodier, 1997, Physical and nutrient variability in the upper equatorial Pacific associated with westerly wind forcing and wave activity, submitted to *Deep Sea Res.*

Harrisson D.E. and B.S. Giese, 1991, Episodes of surface westerly winds as observed from islands in the western tropical Pacific, *J. Geophys. Res.*, 96, 3221 - 3237.

Hellermann, S. and M. Rosenstein, 1983, Normal monthly wind stress over the world ocean with error estimates, *J. Phys. Oceanogr.*, 13, 1093-1104.

Hénin, C. and J. Grelet, 1996, A merchant ships thermo-salinograph network in the Pacific Ocean, *Deep Sea Res.*, in press.

Kuroda, Y. and M.J. McPhaden, 1993, Variability in the western equatorial Pacific ocean during Japanese Pacific climate study cruises in 1989 and 1990, *J. Geophys. Res.*, 98, 4747 - 4759.

Levitus, S., 1982, Climatological atlas of the world ocean, *Rep.NOAA Prof. Paper 13*, NOAA.

Lewis, M.R., M.E. Carr, G.C. Feldman, W. Esaias and C. McClain, 1990, Influence of penetrating solar radiation on the heat budget of the Equatorial Pacific Ocean, *Nature*, 347, 543-545

Lukas, R., 1988, On the role of western Pacific air-sea interaction in the El Niño / Southern Oscillation phenomenon. *Proceedings of the U.S. TOGA Western Pacific Air Sea Interaction Workshop*, Honolulu, 16-18 September, 1987. R. Lukas and P. Webster, U.S. TOGA Rept. USTOGA-8, 43-69.

Lukas, R. and E. Lindstrom, 1991, The mixed layer of the western equatorial Pacific ocean, *J. Geophys. Res.*, 96, 3343-3457.

McPhaden, M.J., F. Bahr, Y. Dupenhoat, E. Firing, S.P. Hayes, P. Niiler, P.L. Richardson and J.M. Toole, 1992, The Response of the Western Pacific Ocean to Westerly Wind Bursts During November 89 to January 90, *J. of Geophys. Res.*, Vol 97, C9, 14289 - 14303.

Oberhuber, J. M., 1988, An atlas based on the COADS data set: the budgets of heat, buoyancy and turbulent kinetic energy at the surface of the global ocean, *Report 15 Max Planck Institut fur Meteorologie*, 20 pp.

Picaut, J. and T. Delcroix, 1995, Equatorial wave sequence associated with warm pool displacements during the 1986-1989 El Niño-La Niña, *Journal of Geophys. Res.*, Vol 100, No C9, 18393 - 18408.

Picaut, J., M. Ioulalen, T. Delcroix, M. J. McPhaden and C. Menkes, 1996, Mechanism of the zonal displacements of the Pacific warm pool: implications for ENSO, *Science*, 274, 1486 - 1489.

Rasmunsson, E.M. and T.H. Carpenter, Variations in tropical sea surface temperature and surface wind fields associated with the southern oscillation / El Niño, *Mon. Wea. Rev.*, 110, 354-384.

Reverdin, G., C. Frankignoul, E. Kestenare and M.J. McPhaden, 1994, Seasonal variability in the surface currents of the equatorial Pacific, *J. Geophys. Res.*, 99, 20323 - 20344.

Reynolds, R. W., 1988, A real time global sea surface temperature analysis, *J. Climate*, 1, 3283-3287.

Roemmich D., M. Morris, W.R. Young and J.R. Donguy, 1994, Fresh equatorial jets, *J. Phys. Oceanogr.*, 24, 540-558.

Sadourny, R. and K. Laval, 1984, January and july performance of the LMD general circulation

model, *New perspectives in climate modelling*, A. Berger Ed., Elsevier, 173-198.

Shinoda, T. and R. Lukas, 1995, Lagrangian mixed layer modelling of the western equatorial Pacific, *J. Geophys. Res.*, 100, 2523-2541.

Smyth, W.D., D. Hebert and J.N. Moum, 1996b, Local ocean response to a multiphase westerly wind burst. 2: Thermal and freshwater responses, *J. Geophys. Res.*, 99, 963-979.

Spencer, R. W., 1993, Global oceanic precipitation from the MSU during 1979-91 and comparisons to other climatologies, *J. Climate*, 6, 1301 - 1326.

Sprintall, J. and M. J. McPhaden, 1994, Surface layer variations observed in multiyear time series measurements from the western equatorial Pacific, *J. Geophys. Res.*, 101, 22513-22532.

Sprintall, J. and M. Tomczak, 1992, Evidence of the barrier layer in the surface layer of the tropics, *J. Geophys. Res.*, 97, 7305-7316.

Tomczack, M., 1995, Salinity variability in the surface layer of the tropical western Pacific Ocean, *J. Geophys. Res.*, 100, 20499 - 20515.

Vialard and Delecluse, 1997a, An OGCM study for the TOGA decade. Part I: Role of salinity in the physics of the western Pacific fresh pool, *J. Phys. Oceanogr.*, 1996.

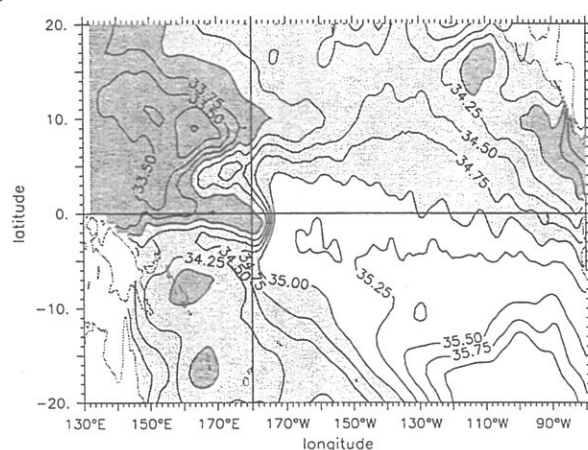**You, Y.**, 1995, A rain formed barrier layer model, *Ocean modelling*, Issue 106, March 1995.

FIGURES (*Annexe B*)
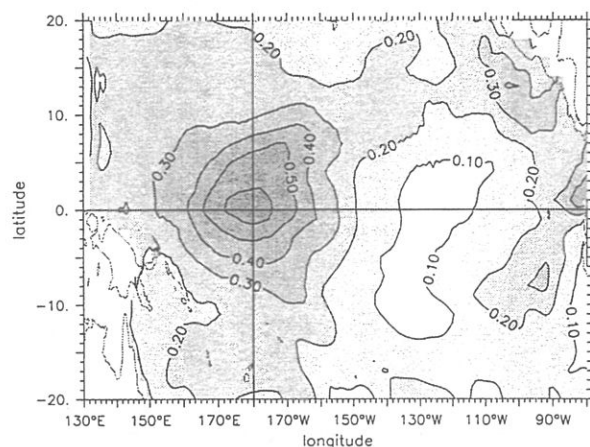
Figure B.1. Root mean square of the 5 day averaged SSS of the control experiment over the 1985 - 1994 period. Contour interval is 0.1 psu.
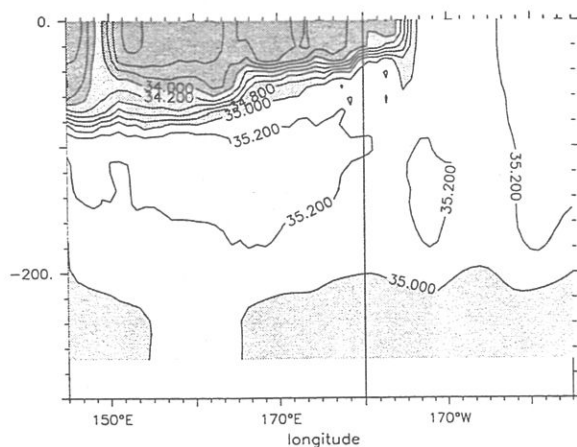
Figure B.2. Longitude depth section of the simulated SSS during the last week of october 1990. Contour interval is 0.1 psu.
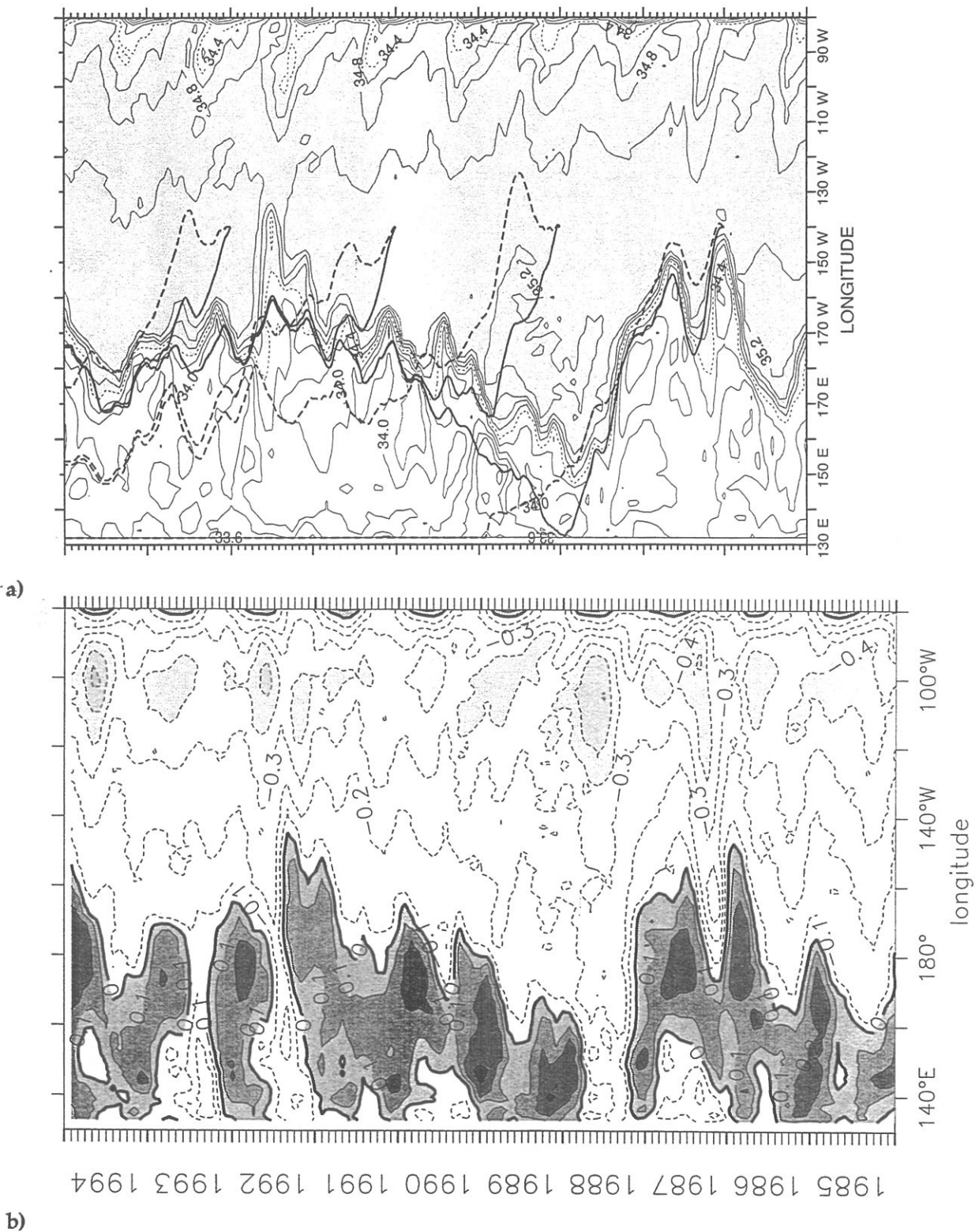

Figure B.3. Map of the simulated SSS during the last week of october 1990. Contour interval is 0.25 psu.

a)
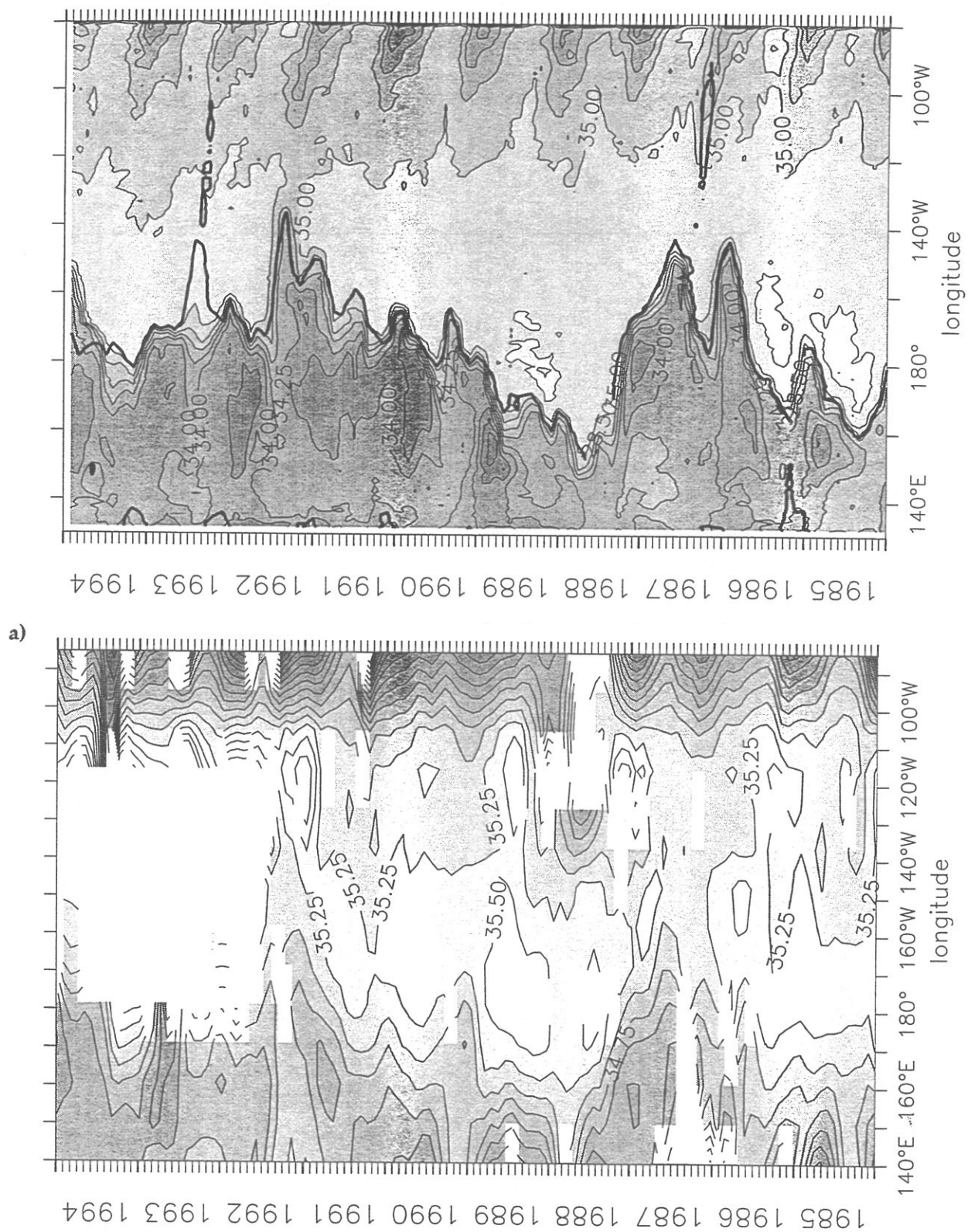
b)

Figure B.4. Time longitude evolution of the SSS in the 2°N - 2°S band. (a) From the control experiment. (b) From data along four navigation tracks. Units are in psu. Contour interval is 0.25 psu.

a)

b)

Figure B.5. Time longitude evolution in the 2°N - 2°S band of: (a) SSS and trajectories of an hypothetical 4°N - 4°S drifter advected by the surface (continuous line) and 70 meters (dashed line) zonal currents. (b) Zonal current at 5 meters minus zonal current at 71 meters. Units and contour interval are in (a) psu and 0.2 psu and (b) meters/second and 0.1 ms^{-1}.

a)

b)
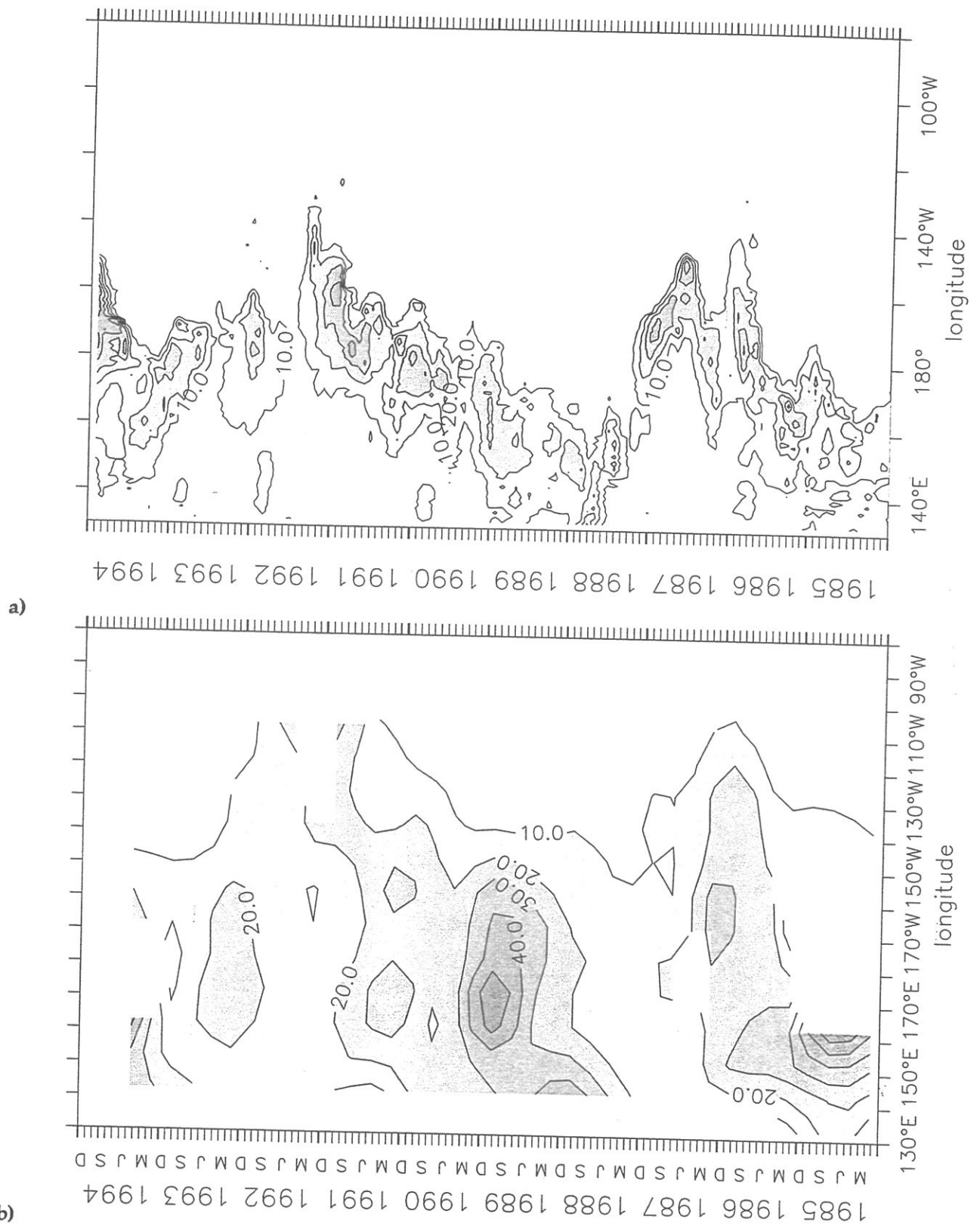
Figure B.6. Time longitude evolution in the 2°N - 2°S band of (a) BLT of the control experiment. (b) observed BLT from AM.

a)

c)

b)

d)
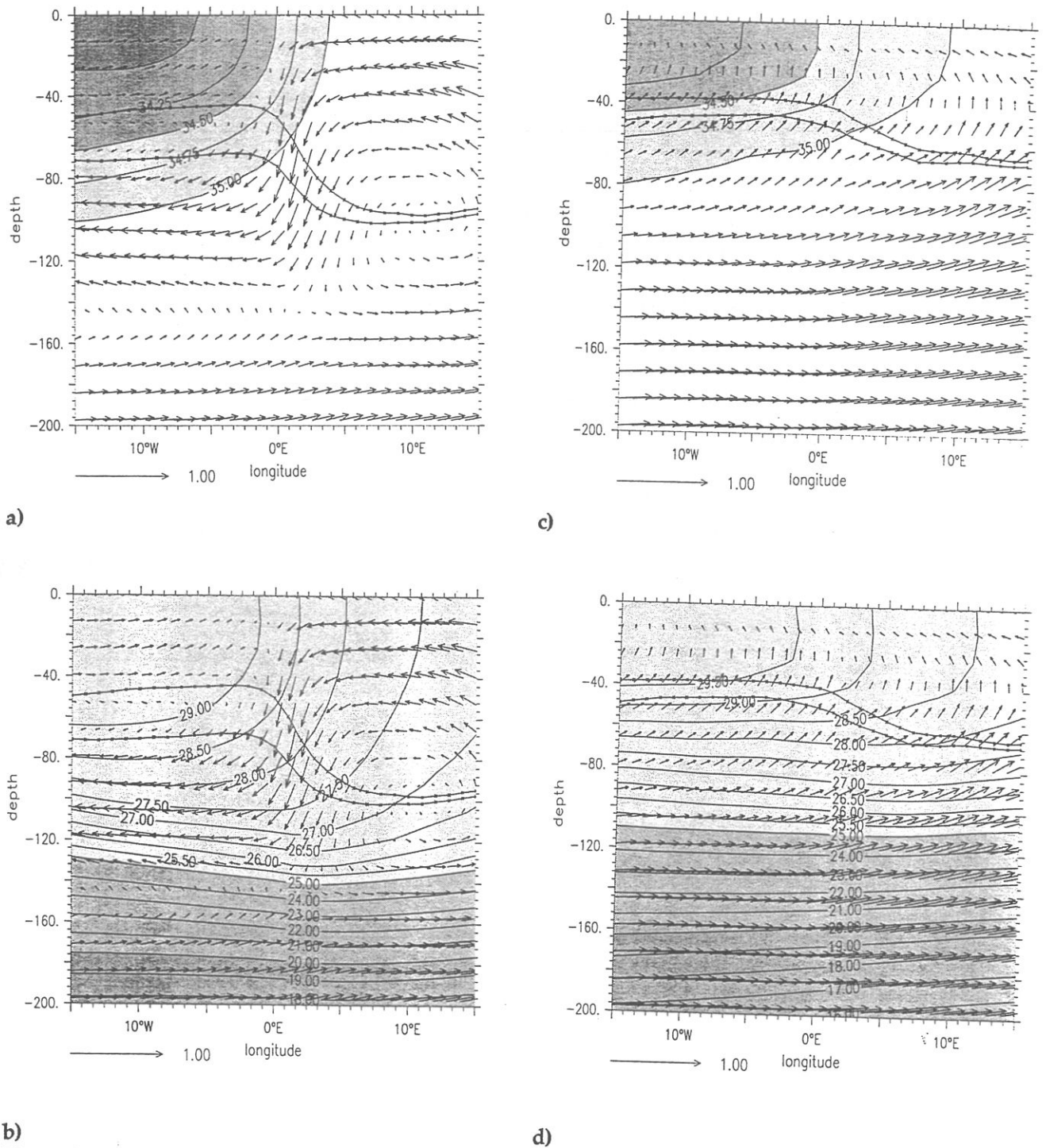
Figure B.7. Depth longitude section of simulated hydrographical structure at the equator near the front (longitude in the horizontal axis is relative to the front position). (a) Currents (vectors) and Salinity (contouring) averaged over the months where the mean BL west of the front is greater than 10 meters. (b) Idem with temperature. (c) Same as (a) but when no significant BL appears west of the front. (d) Same as (b), when no significant BL appears west of the front. Unit vector is given in $m.s^{-1}$ for zonal speed. The maximum vertical speed in figures a and b is around 1.5 $m.day^{-1}$. Contour interval is 0.1 psu for salinity and 1°C / 0.5 °C for temperatures under / above 25°C.
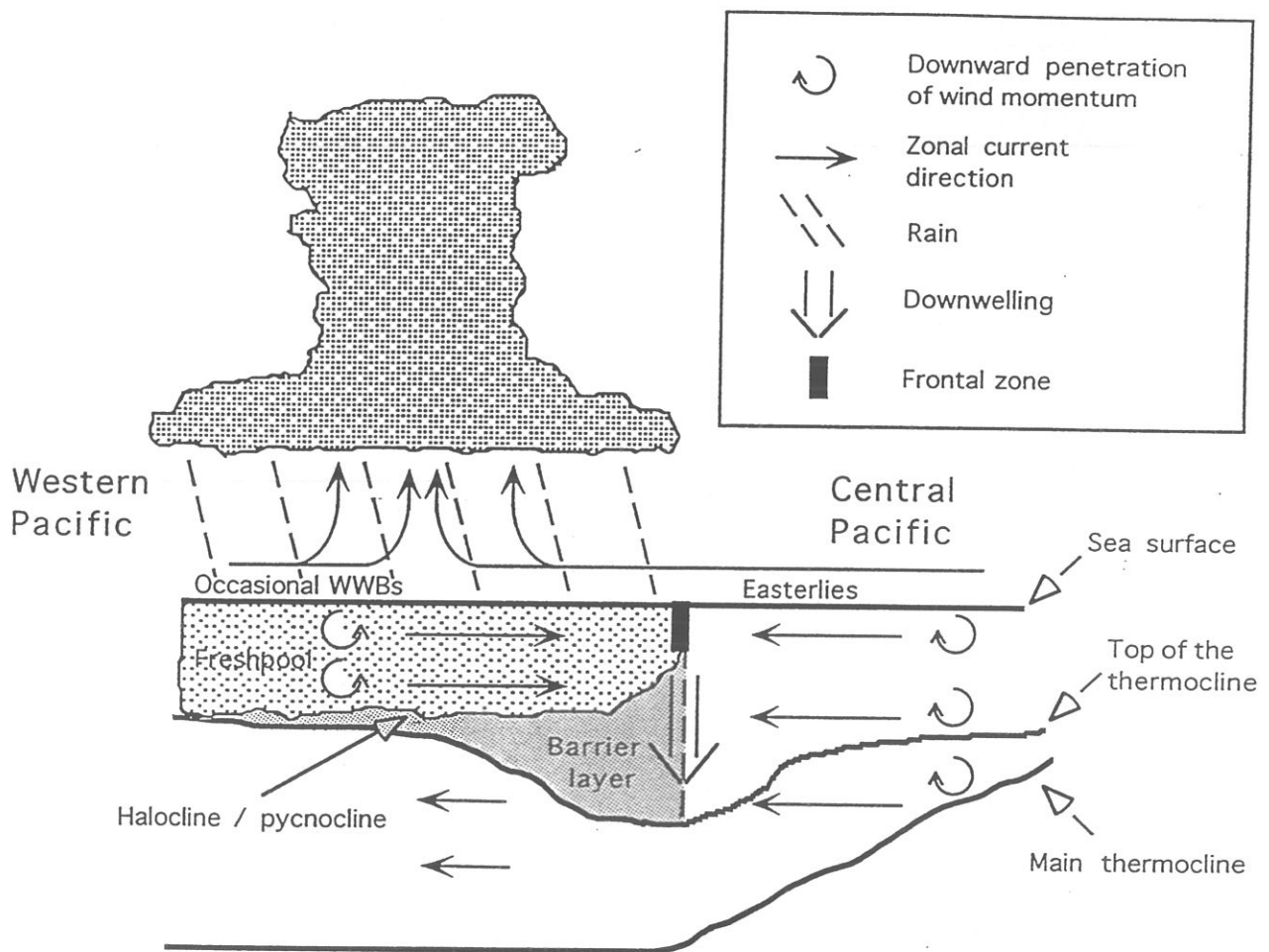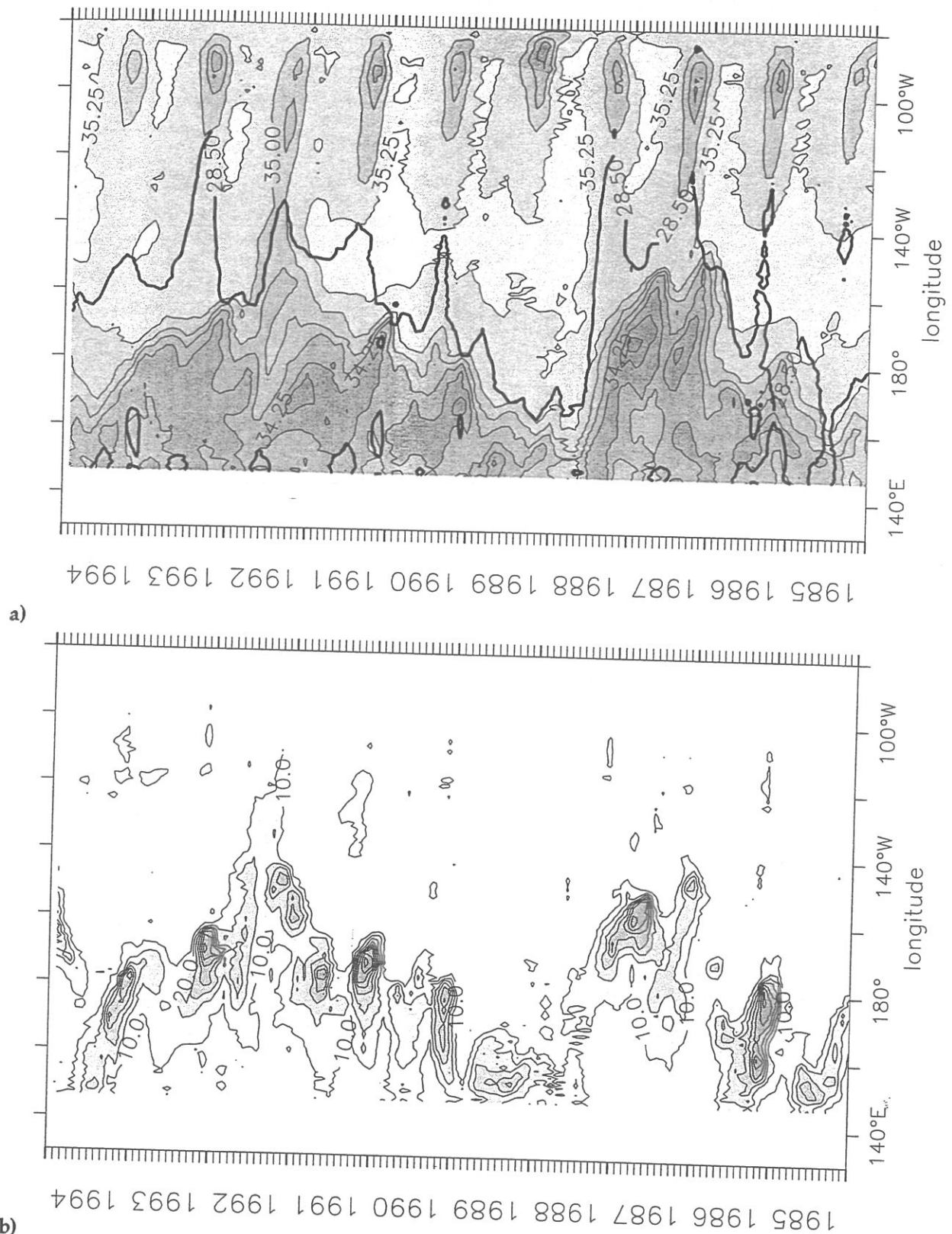
Figure B.8. Schematic view of a longitude depth section of the SSS frontal zone region.
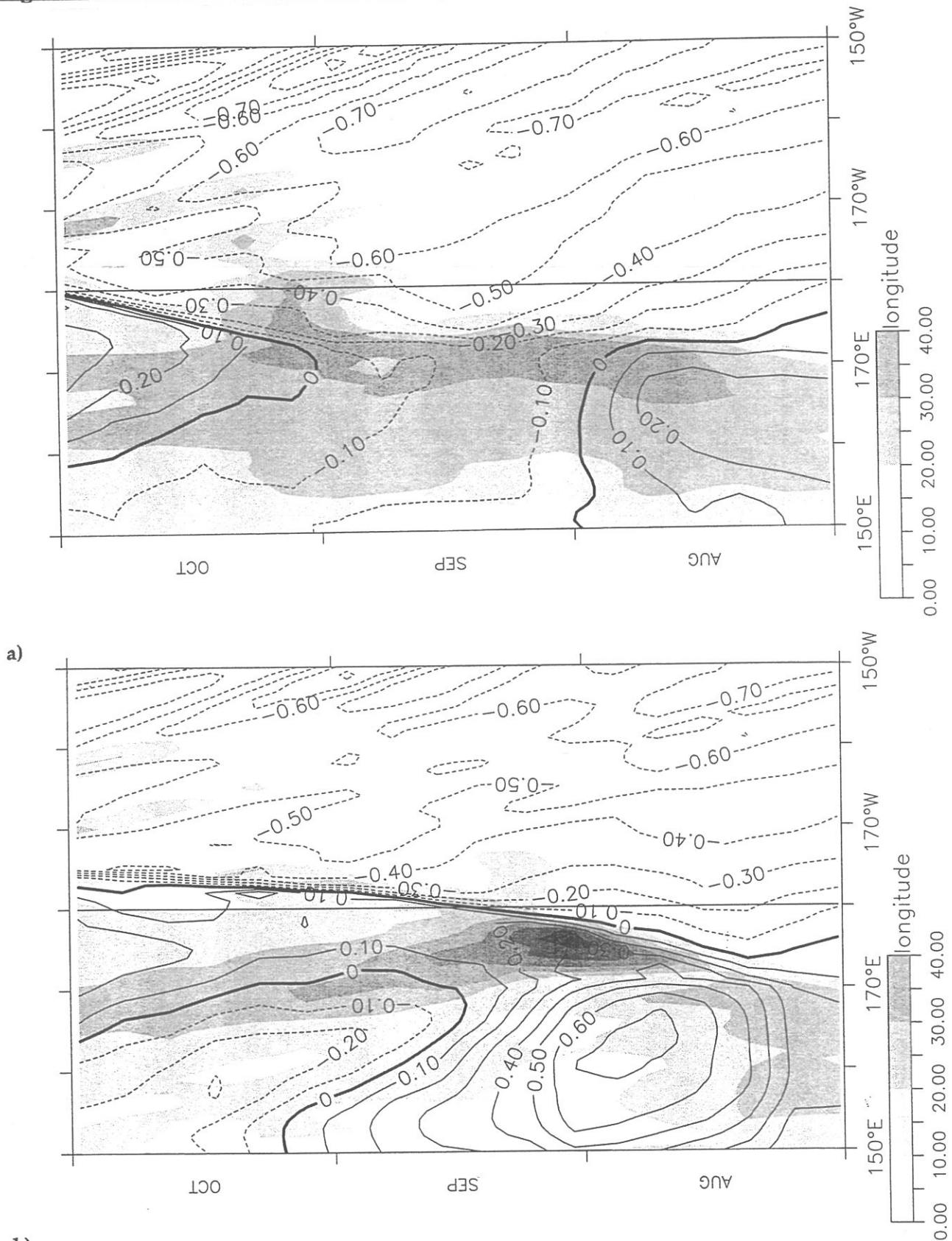
Figure B.9. Simulated BLT (grey tones) and zonal currents (contouring) for (a) control experiment and (b) wind burst experiment. Unit are in meters for BLT and m.s^{-1} for zonal speed. Contour interval for zonal speed is 0.2 m.s^{-1}.

a)

b)

Figure B.10. (a) Time longitude evolution in the 3°S - 6°S band of (a) simulated SSS, (b) simulated BLT. Units are in psu (SSS) and meters (BLT). Contour interval is 0.25 psu for SSS and 10 m for BLT. The 28.5°C isotherm has been overlaid to the SSS plot.
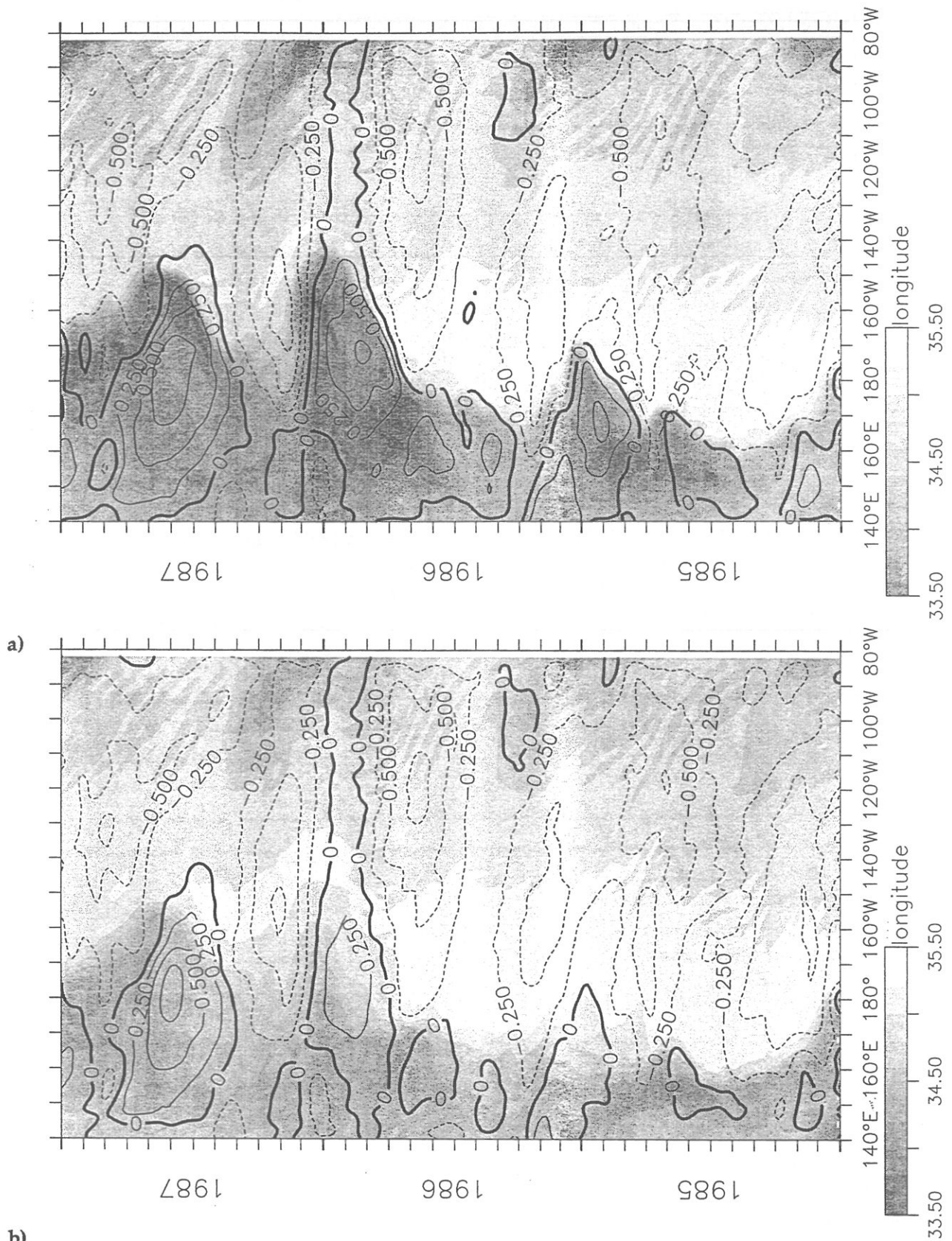
a)

b)
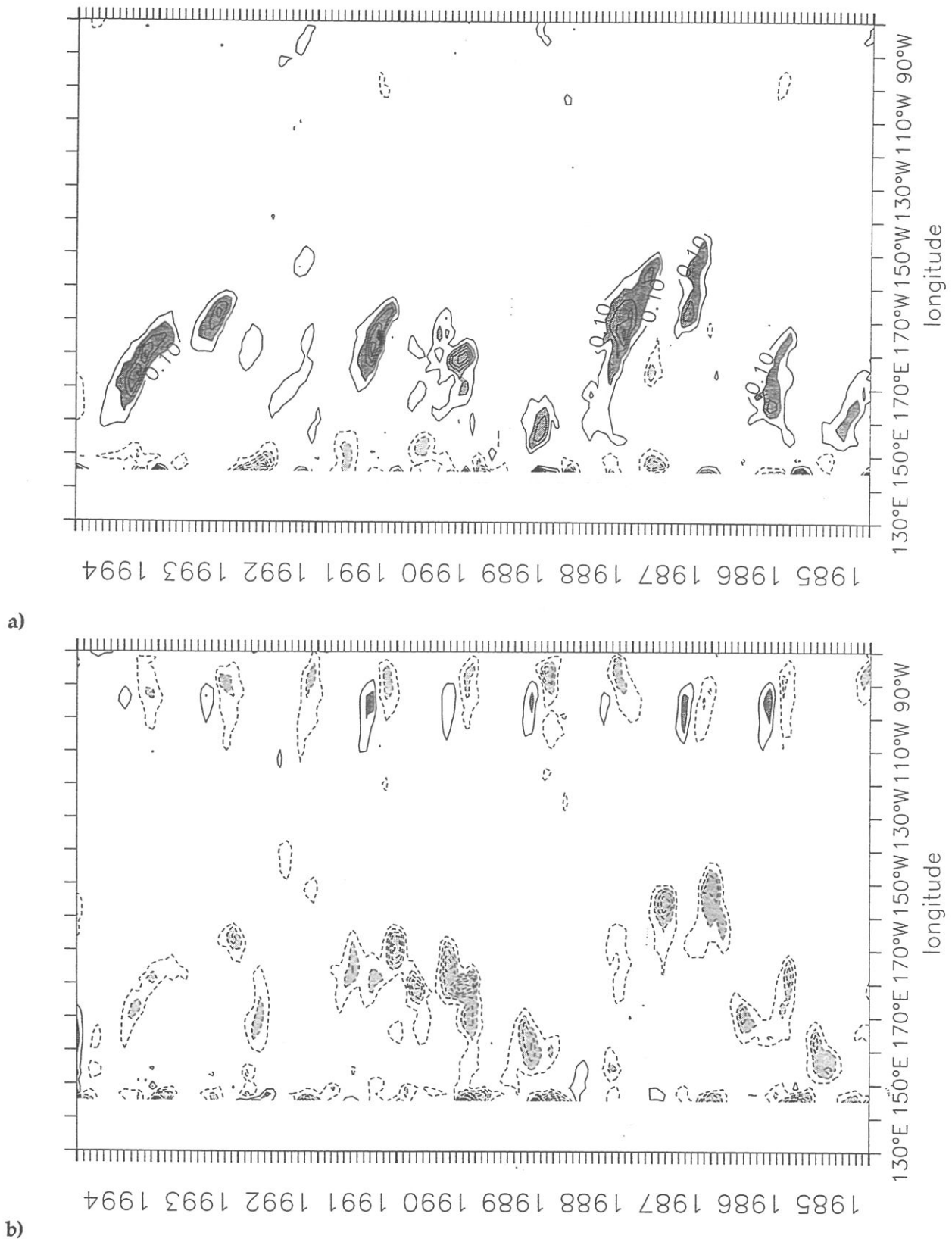
Figure B.11. Time longitude evolution in the 3°S - 6°S band of (a) mixed layer salinity zonal advection term and (b) mixed layer salinity meridional advection term. Units are in psu/month. Contour interval is 0.1 psu/month with zero contour not shown.
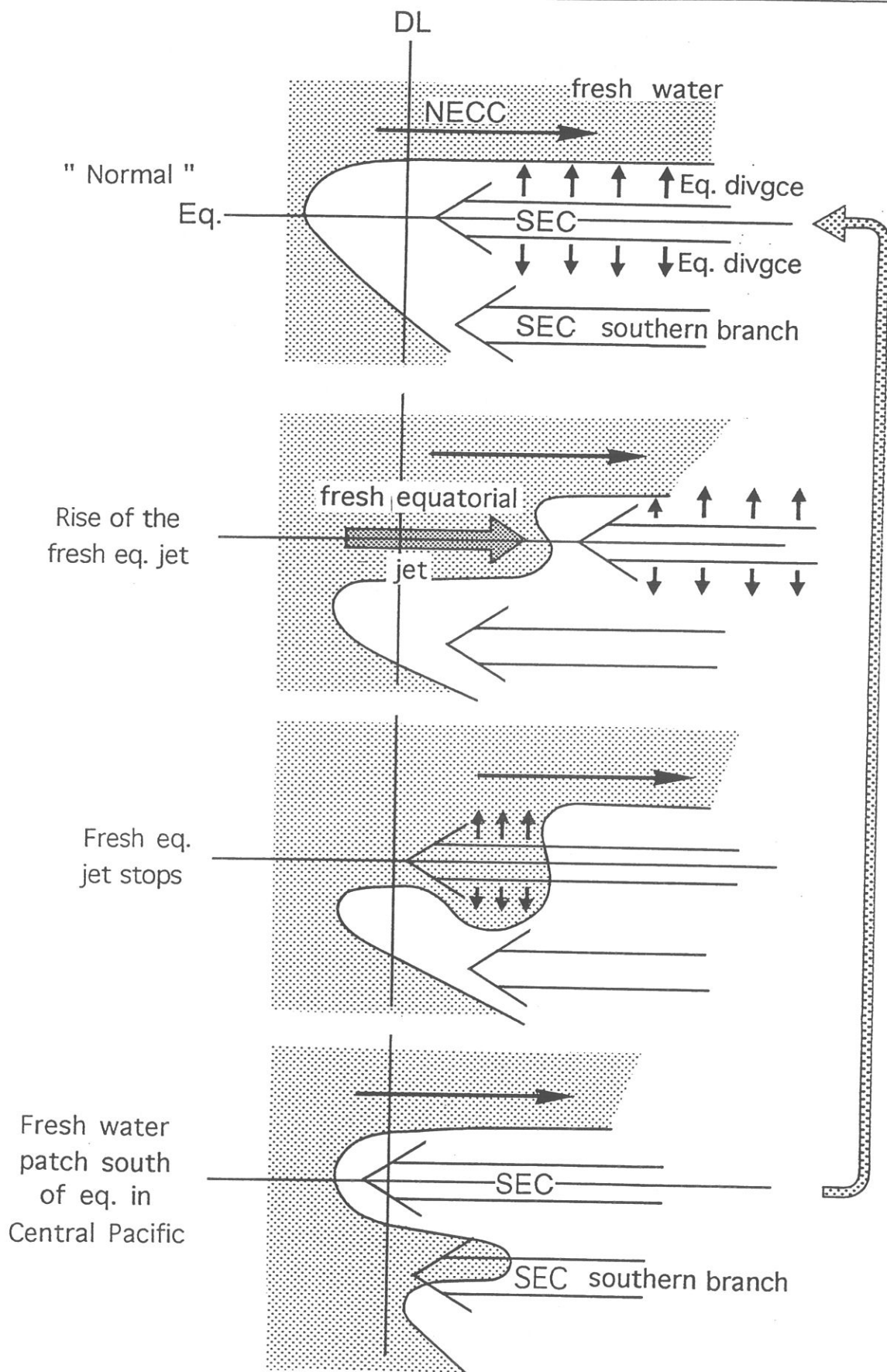
Figure B.12. Schematic representation of the freshwater meridional advection after an equatorial jet.

Influence de la salinité sur les interactions océan - atmosphère dans le Pacifique tropical.

a)

b)

Figure B.13. Time longitude evolution of superimposed SSS (shades of grey) and zonal current (contouring) in the 2°N - 2°S band. (a) Standard experiment. (b) A1 experiment. Units are in ms^{-1} (zonal current) and psu (salinity). Contour interval is 0.25 ms^{-1}.

Experiment	Resolution	Forcing fields	Vertical diffusion
C (Standard)	TDH (medium resolution)	Arpege wind stress Arpege heat flux Arpege water flux	f(T,S)
A1	TDH	Idem	f(T,35‰)
A4	TDH	Arpege wind stress Arpege heat flux LMD water flux	f(T,S)
H1	TOTEM (high resolution)	Arpege wind stress Arpege heat flux Arpege water flux	f(T,S)
H2	TOTEM	ECMWF wind stress ECMWF heat flux Arpege water flux	f(T,S)
W0	TDH	Annual Arpege wind stress Annual Arpege heat flux Annual Arpege water flux	f(T,S)
W1	TDH	Annual Arpege wind stress + wind burst Annual Arpege heat flux Annual Arpege water flux	f(T,S)

Table B.1. Summary of the sensitivity experiments referenced in this paper.

Trends units: psu/month * 1000	West of front	Front -> East	Front -> West	East of front
Zonal advection	-9	-351	272	6
Meridional advection	-64	-231	-132	-10
Vertical advection	-5	17	5	5
Horizontal diffusion	25	26	8	-3
Forcing	-238	-161	-143	-8
Entrainment	281	298	195	34
Salinity (psu)	33.96	34.6	34.6	35.14

Table B.2. Values of mixed layer salinity tendency terms integrated around the salinity front. The position of the front (x_f) is defined as the position of the 34.6 isohaline. The western zone is defined as $[x_f-15°,x_f-5°[$, the frontal zone as $[x_f-5°,x_f+5°]$, the eastern zone as $]x_f+5°, x_f+15°]$. Tendency terms are given separately for eastward and westward propagations in the frontal zone. Tendency terms are in psu/month.

	Period	MLD (m)	BLT (m)	Qnet (W/m2)	Ax (W/m2)	Ay (W/m2)	Az (W/m2)	Dh (W/m2)	F (W/m2)	E (W/m2)
Box 1 2°N-2°S 140 - 160°E	87, El Niño Far western	37	~ 0	22	-2	7	0.5	-1	3	-10
	89, La Niña Western	35	17	16	-2.5	0.5	-0.5	-0.5	0	3.5
Box 2 2°N-2°S 170 - 180°E	88.5- 89.5, La Niña Central	63	~ 0	63	-24.5	9	-3	-0.5	61.5	-47
	91, El Niño Western	40	24	20	-4.5	3.5	-0.5	-1	5.5	-0.5

Table B.3. Averaged values of net heat flux, mixed layer depth and mixed layer temperature tendency terms over Boxes I, II in "central", "western" or "far western" Pacific situations. Ax: zonal advection. Ay: meridional advection. Az: Vertical advection. Dh: Horizontal diffusion. F: Atmospheric forcing. E: Entrainment. Tendency terms are given in °C/month.

Influence de la salinité sur les interactions océan - atmosphère dans le Pacifique tropical.

Déjà paru :

1 : Janvier 1998 Agnès Ducharne, Katia Laval and Jan Polcher, *Sensitivity of the hydrological cycle to the parameterization of soil hydrology in a GCM*

2 : Janvier 1998 Marina Lévy, Laurent Mémery and Jean-Michel André , *Simulation of primary production and export fluxes in the Northwestern Mediterranean Sea*

3 : Février 1998 Valérie Masson, Sylvie Joussaume, Sophie Pinot and Gilles Ramstein, *Impact of parameterizations on simulated winter mid-Holocene and Last Glacial Maximum climatic changes in the Northern Hemisphere*